DILUENT EFFECTS ON DIFFUSION FOR THE SYSTEM URANYL NITRATE-TRIBUTYL PHOSPHATE-N-HEPTANE

By

AMABLE D. HORTAÇSU

Bachelor of Science
University of the Philippines
Diliman, Q. C., Philippines
1963

Master of Science
Oklahoma State University
Stillwater, Oklahoma
1965

Submitted to the Faculty of the
Graduate College of the
Oklahoma State University
in partial fulfillment of
the requirements for
the Degree of
DOCTOR OF PHILOSOPHY
July, 1970

DILUENT EFFECTS ON DIFFUSION FOR THE SYSTEM URANYL NITRATE-TRIBUTYL PHOSPHATE-N-HEPTANE

Thesis Approved:

John B. West
Thesis Adviser

Robert S. Robinson, Jr.

John H. Huba

Tom E. Moore

D. Dunham
Dean of the Graduate College

PREFACE

This study is an effort to examine some diluent effects and the solute concentration dependence of diffusion rates in uranyl nitrate-tributyl phosphate-n-heptane system. It is also aimed to add qualitatively to existing studies leading to the understanding of the molecular interactions present in the system.

I would like to thank many people who made this study possible. Sincere gratitude is extended to Dr. John B. West for his guidance as thesis adviser and for encouragement in the course of my graduate work. I also wish to thank Dr. Calvin Slater, who established many experimental procedures for this work, and Mr. Patrick Metz for valuable discussions. Appreciation is expressed to Mr. Eugene McCroskey for his help in securing needed materials. I am also grateful for helpful comments extended by my advisory committee, Dr. R. L. Robinson, Dr. J. H. Erbar and T. E. Moore.

I am very grateful to many women of the P.E.O. for a two-year International Peace Scholarship. I am also indebted to the United States Atomic Energy Commission for funds under Contract AT(11-1)-846 for the purchase of materials, equipment and for financial support.

I wish to thank my husband, Öner, for many valuable suggestions on the thesis and for his patience and understanding which made the completion of this work possible. Most of all, I am indebted to my late father, my mother, my brothers and sisters who shared many of my dreams and gave me support and encouragement to pursue them.

TABLE OF CONTENTS

LIST OF TABLES

LIST OF FIGURES

CHAPTER I

INTRODUCTION

Uranium recovery is an important function of nuclear processing plants. Recovery is accomplished by the solvent extraction of the active material into an organic solution. The engineering as well as the chemical aspects of this extraction process has been the subject of numerous studies.

The use of tributyl phosphate (TBP) as an extractant requires the addition of a diluent to facilitate handling. The choice of the diluent is important since it has been observed that the nature of even so-called "inert" diluents such as hydrocarbons and their derivatives may affect the rate of extraction. Studies made to explain this diluent effect have led to the more fundamental examination of the physico-chemical and thermodynamic properties of the organic solutions formed.

Hand in hand with industrial mass transfer operations is the growing body of investigations on transport processes in multicomponent systems. At present, no completely satisfactory theory exists and little experimental data is available to test whatever theory has been forwarded.

It was with this background that the research project presented here was initiated. The purpose was to study the

diffusion of uranium in tributyl phosphate-diluent solutions with respect to two variables; namely, the degree of dilution of the tributyl phosphate solvent and the uranyl nitrate concentration. N-heptane was chosen as a typical saturated hydrocarbon diluent. Experimental diffusion coefficient data were gathered, using a birefringent interferometer, for uranyl nitrate in 30 V/V percent TBP-n-heptane, 50 V/V percent TBP-n-heptane and 70 V/V percent TBP-n-heptane. The concentration range up to near saturation with respect to uranyl nitrate, was covered in each solvent mixture.

CHAPTER II

REVIEW OF LITERATURE

The review of literature is divided into two parts. The first part deals with the contributions to the physical and chemical characterization of the system uranyl nitrate-tributyl phosphate-diluent and the second part deals with the more general subject of techniques and theories of diffusion as applicable to this study.

The System Uranyl Nitrate-Tributyl Phosphate-n-Heptane

Three aspects of the available literature about the uranyl nitrate-tributyl phosphate-n-heptane system are of interest in this study. They are, diluent effects in extraction, thermodynamic studies and diffusion measurements made on the system. These are discussed briefly in the following paragraphs.

Diluent Effects in Extraction

In the extraction of uranyl nitrate from an aqueous solution by tributyl phosphate (TBP), the addition of a diluent is necessary in order to obtain a solvent phase of suitable density and sufficiently low viscosity. For this

purpose, inert diluents, usually saturated or aromatic hydrocarbons and their halo derivatives are added.

The effect of the diluent on the distribution of uranyl nitrate between the tributyl phosphate and aqueous phases is the subject of a large number of studies.

The mechanism of uranyl nitrate extraction was first proposed by Moore (47) as follows:

$$UO_{2(aq)}^{++} + 2NO_3^- + 2TBP \rightleftharpoons UO_2(NO_3)_2 \cdot 2TBP_{(org.)} \qquad (II-1)$$

An equilibrium constant for this reaction may be written as:

$$K = \frac{[UO_2(NO_3)_2 \cdot 2TBP]\,\gamma_{U2T}}{[UO_2^{++}][NO_3^-]^2\,\gamma_{\pm}^3[TBP]^2\,\gamma_{TBP}^2} \qquad (II-2)$$

where the use of brackets indicates concentration units and γ's are the activity coefficients.

The distribution ratio, defined as the ratio of the concentration uranyl nitrate present in the organic phase to that in the aqueous phase is described by:

$$K_D = \frac{[UO_2(NO_3)_2 \cdot 2TBP]_{org}}{[UO_2^{++}]_{aq}} \qquad (II-3)$$

for which we obtain:

$$K_D = \frac{K[NO_3^-]^2 \gamma_{\pm}^3 [TBP]^2 \gamma_{TBP}^2}{\gamma_{U2T}} \qquad \text{(II-4)}$$

If both phases are considered ideal, at constant aqueous phase concentration, the distribution ratio increases as the square of the am ount of tributyl phosphate in the solvent.

Studies on the effect of the nature of diluents on the distribution ratio led to numerous publications and equally numerous conflicting conclusions. Burger (13), in his early comparative study of diluents for tributyl phosphate, concluded that the differences in distribution ratio among hydrocarbons and certain chlorinated hydrocarbons was insignificant. Others, (48, 53, 64, 65) later showed that on the whole, diluents may be arranged with respect to the degree of their influence on the distribution ratio. These studies established that the distribution ratio is greater in the case of aromatic and aliphatic hydrocarbons than for their halogen derivatives. Shevchenko (64) noted that among aliphatic hydrocarbons, the distribution ratio decreased with increasing number of carbon atoms in the chain, and among benzene derivatives seemed to decrease with increasing number of methyl groups. Especially low distribution ratio values were obtained by Pushlenkov (53) and Healy (33) for chloroform used as diluent.

Many attempts have been made to correlate these observations with the physicochemical properties of the diluent. Shevchenko (64, 65) connected the extractability by TBP

with the dielectric constant and polarizability of the diluent. On the other hand, Pushlenkov et. al. (53) did not observe any correlation between the extraction by TBP and dielectric constant, dipole moment or refractive index of the diluent. Taube (75) proposed that although the extractability cannot be related in a simple way to the diluent polarity, it is indeed an important factor if viewed in the following manner: (1) interaction between the dipole of the organic complex and the diluent dipoles favor extractability and (2) mutual interaction between the dipoles in the diluent molecules give rise to a "structure" in the organic phase, which hinders extraction. In the case of slightly polar complexes with TBP, like the uranyl nitrate complex $UO_2(NO_3)_2 \cdot 2TBP$ the second effect is stronger, and extraction into polar diluents is lower than the extraction into non-polar ones. Related to the concept of permanent or induced diluent dipole which hinders extraction, Healy (33) observed a decrease of the distribution ratio with an increase in the water solubility in the pure diluent.

Although the role of the nature of the diluent on the extraction is unambiguously related to the physical constants of the diluents, a definite quantitative correlation has not yet been established.

On returning to the basic thermodynamic equation for the distribution ratio, further works (54, 56, 67) led to the proposal that the influence of the nature of the diluent

is determined by two competing interactions; interaction of the diluent molecules with the molecules of the extraction reagent on one hand, and interaction of the diluent molecules with the molecules of the extracted complex on the other. The quantitative treatment of these interactions is reduced to the determination of the activity coefficients of the complex and the extraction reagent in the organic phase. Vdovenko (79) used the theory of regular solutions to calculate the activity coefficients and derived an expression for the distribution ratio dependent on the solubility parameter and molar volume of the diluents. Pushlenkov (55), Apelblat (2) and Rozen (62) determined the activity coefficients of the binary systems, complex-diluent and TBP-diluent for a number of representative class of diluents. Their data indicate that the system cannot be described rigorously by the theory of regular solutions.

A quantitative expression for the effect of the nature of the diluent in extraction is closely tied with the liquid solution theory describing the system. More work must be undertaken in this direction.

The Nature of the Uranyl Nitrate-Tributyl Phosphate-Diluent System

An exhaustive compilation of the properties of tributyl phosphate relevant to solvent extraction is given by McKay and Healy (45). After purification, as it is commonly used, TBP is saturated with water. The solubility

of water in 100% TBP at 25°C is reported at 64 and 58 g/l (16). A nearly 1:1 mole ratio is pointed out and has led to some studies (3, 39, 60) to ascertain whether or not a compound TBP·H_2O complex does exist but is only weakly bonded (60). The addition of a hydrocarbon diluent to tributyl phosphate causes the water solubility to drop. The water content falls well below the 1:1 mole ratio observed for higher TBP dilutions (14).

The extraction of $UO_2(NO_3)_2$ by TBP from an aqueous solution or the dissolution of solid uranyl nitrate hexahydrate in TBP is the result of the formation of a uranyl nitrate-TBP complex (47).

The value of the reaction equilibrium constant at 25°C has been determined by several authors (1, 21, 32, 61, 66). Equilibrium constants expressed in molar concentration, K_c, and in molal concentration, K_m, are given by Sidall (66) ($K_c = 90$), Healy (32) ($K_m = 2230$), and Rozen and Khorkhorina (61) ($K_c = 30$-70) and Aartsen and Korveze (1) ($K_c = 48$). Davis and Mrochek (21) using some determined activity data and a curve fit analysis found an equilibrium K value of 2650. This value is not directly comparable with the ones previously given because the K value in the latter is based on mixed activity units.

The heat of reaction for the complex formation, which is exothermic, was determined calorimetrically at 6300 cal/mole by Nikolaev (49).

Studies on the partition coefficient (1, 35, 47), absorption spectra analysis (42) and conductometric determinations in the organic phase (35, 77) established that the uranyl nitrate occurs in the organic solution as an anhydrous, practically undissociated molecule of the form $UO_2(NO_3)_2 \cdot 2TBP$. The specie is the same for all hydrocarbon and chlorinated hydrocarbon diluents used, and the ratio 1 mole uranyl nitrate to every 2 moles tributyl phosphate is not altered by dilution.

The addition of uranyl nitrate drastically reduces the water content of the tributyl phosphate-diluent solution. With 100% tributyl phosphate, Healy (35) approximates that every molecule of uranyl nitrate displaces two of water. In tributyl phosphate-diluent solutions, Burger (14) noted that the water content of such solutions follows the concentration of free tributyl phosphate.

Chemical studies (12) have shown that in the presence of alkalis, acids and water, tributyl phosphate hydrolyzes to form dealkylated products such as dibutyl phosphate, monobutyl phosphate and phosphoric acid. The most significant degradation product is the dibutylphosphate. At 25°C, in water saturated TBP, the degradation reaction is first order with respect to TBP concentration with a rate constant of $k_D \doteq 2 \times 10^{-7}$ per hour. Dibutyl phosphate forms a complex with uranyl nitrate, which is quite soluble in TBP-hydrocarbon mixtures. Although uncertain, most experimental work (12) seems to conclude that uranyl nitrate has

a negligible effect on the decomposition of TBP if the solution is not exposed to light.

The systems uranyl nitrate-tributyl phosphate-diluents form non-ideal solutions. The deviations from ideality are the result of the $UO_2(NO_3)_2 \cdot 2TBP$ plus diluents, TBP plus diluents and TBP plus $UO_2(NO_3)_2 \cdot 2TBP$ interactions. Activity coefficient measurements have been made (2, 21, 34, 55, 62) for some representative binary systems in order to determine the extent of the interactions. The binary systems $UO_2(NO_3)_2 \cdot 2TBP$ plus aliphatic hydrocarbon, TBP plus aliphatic hydrocarbon exibit positive deviations from ideality (2, 55, 62). The rational activity coefficient of the dissolvate $UO_2(NO_3)_2 \cdot 2TBP$ in n-hexane has a value from 1 to 5 (55). Pushlenkov (55) and Rozen (62) conclude that the interaction in the presence of systems like hexane is due only to Van-der-Waals forces. Negative deviations are exhibited by systems with $CHCl_3$, CCl_4 and benzene (55, 62). Because of the marked differences in the dimensions of the molecules of the disolvate, TBP and diluent, the athermous effect has been used (62) to account for the negative nonidealities. Association effects have also been considered for these systems. Davis and Mrochek (21) calculated the molar activity coefficients for the binary system $UO_2(NO_3)_2 \cdot 2TBP$-TBP from equilibrium data. Calculated values of 1.0 to 4.0 are given.

Healy et. al. (34) have made some vapour pressure measurements for the system $UO_2(NO_3)_2$-TBP-CCl_4 binary sys-system. The data seem to indicate that the partial pressure of TBP was unaffected by the presence of uranyl nitrate. However, the concentration of uranyl nitrate was not indicated, the concentration of TBP was given in mole fractions based on a TBP-CCl_4 binary scale. The vapour pressure data were probably for a trace concentration of uranyl nitrate.

The state of thermodynamic studies on the uranyl nitrate TBP-diluent system although numerous is far from satisfactory. Earlier experimental activity coefficient data tend to show that the binary combinations of the components may be represented by the equation for regular solutions. Current measurements and correlations tend to contradict and suggest far more complicated expressions. To date, there is no available thermodynamic data for the ternary system uranyl nitrate-tributyl phosphate-diluent.

Diffusion Studies on the System

Three studies (25, 30, 50) have dealt with measurements of the diffusion coefficients of uranyl nitrate in tributyl phosphate - Amsco solution. All of the data presented were obtained by the capillary cell technique.

Hahn (30) reported diffusion coefficients at 25°C for 0.44M UN in 30% TBP-Amsco and 1M UN in 71% and 100 % TBP-Amsco. The diffusion coefficients obtained by Finley (25)

were higher than those obtained by Hahn(30).

A study of the molecular dimension of the uranyl nitrate tributyl phosphate complex was made by Nicolaev (50). The radius was determined from the Nernst-Einstein relation (42) using diffusion data reported by Hahn (30) and two other points taken at 20°and 18°C. He found that the viscosity product, $D\mu$, hence the calculated radius of the molecule, varied with the concentration of the solution.

At present, no comprehensive study of the diffusion of uranyl nitrate in organic solution exists. All of the previous work reported were at randomly picked uranyl nitrate concentrations, the main purpose of the studies being to determine order of magnitude values of the diffusion coefficient. Furthermore, no attempt has yet been made to examine the effect of the diluent on the diffusion coefficient.

Diffusion

The following is a brief summary of contributions to birefringent interferometry and some theories of liquid diffusion pertinent to this study.

Diffusion Measurement from Birefringent Interferometry

The quantitative measurement of path differences and gradients by means of interference effects produced in a Savart Plate, was first introduced by Ingelstaam (37). The core of the method consists of splitting a ray of plane

polarized light into two rays by a Savart plate. The phase difference (introduced in the optical path, i.e. diffusion cell) between two rays emerging at the same spot from the Savart plate, but originating from different parts of the entering wave front, is detected by a suitable analyzer.

The Savart plate is a double crystal, each crystal cut in such a way that the normal of the plates makes an angle of 45° with respect to the optical axes of the crystal. The two square plane-parallel plates are mounted together with their optical axes turned 90° with respect to each other (73). In the Savart plate a pencil of polarized light is divided into two rays, displaced with respect to one another a distance "b " and vibrating perpendicularly to one another. The value of "b" depends on the angle of incidence between the wave front and the plane of the Savart plate. If the entering ray traverses the Savart plate perpendicularly, the displacement "b" is a function only of the thickness of the plates and the principal refractive indices (38). Ingelstaam (38) and Bryngdahl (8) give a detailed description of the shearing of the entering wave front through the Savart plate.

The resulting wave fronts interfere destructively or constructively according to their path difference. A polarizer mounted such that its polarization direction is either perpendicular or parallel to the polarization direction of the light source produces the desired horizontal

interference pattern. Skinner (68) described by vector equations the formation of interference fringe patterns.

Bryngdahl (8) has developed the method for studying diffusion in dilute liquid solutions. To date three variations (8, 9, 10) have been introduced. The first variation which employs one Savart plate produces horizontal fringe pairs, the second, with two Savart plates result in interference fringes which are a direct plot of the refractive index gradient. Since the resulting refractive index gradient is not plotted in the cartesian coordinate system, x, y of the plate, a modified double crystal plate is used for the third variation.

The first and simplest arrangement was used in this study. The optical arrangement of Bryngdahl's birefringent interferometer using one Savart plate is shown in Figure 1. A mercury arc lamp with a monochromator was used a light source. A flowing junction type diffusion cell was used. The Savart plate was mounted perpendicular to the optical axes of the arrangement, in this way, the emerging rays are equally strong. The Savart plate was tilted a slight amount to obtain fringes for very dilute solutions. The diffusion runs were carried out at room temperature.

Bryngdahl (8) has outlined several methods for calculating diffusion coefficients from the resulting fringe pattern. From Fick's first law of diffusion (8, 17), the flux with respect to a fixed reference frame, i.e., at the interface, N_1, is given by:

E - LIGHT SOURCE
L - LENS
S - SAVART PLATE
P - POLARIZER
M - IMAGE PLANE

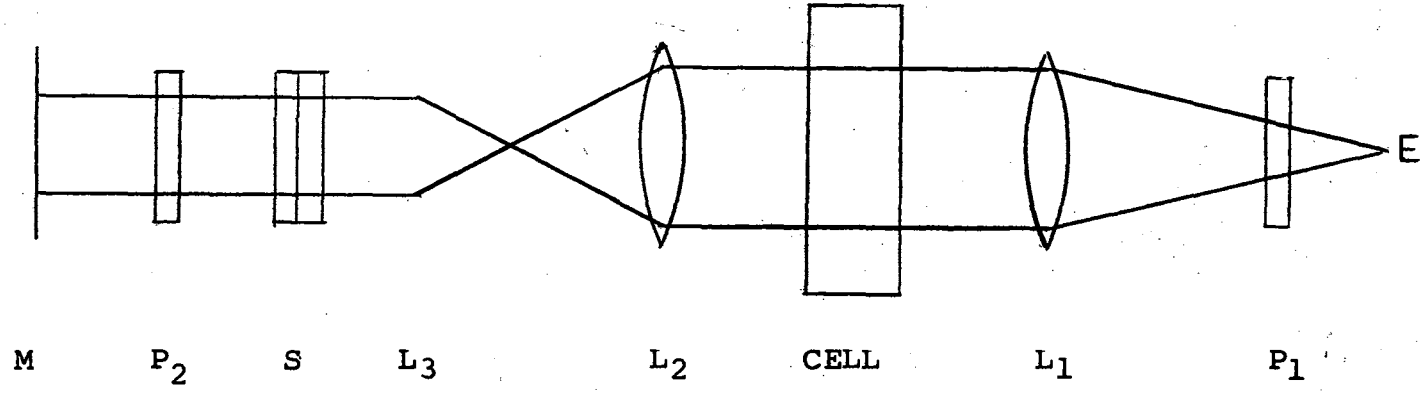

Figure 1. Optical Arrangement of One Savart Plate Interferometer Used by Bryngdahl (8)

$$N_1 = -D\frac{\partial C_1}{\partial x} \qquad \text{(II-5a)}$$

For the following conditions: (1) the diffusion coefficient D is a constant, (2) the dimension of the cell in the direction of diffusion is infinite in extent and (3) the diffusion starts from an initially sharp interface, i.e., the initial condition at x=o is a step function in concentration; the solution to Equation (II-5a) is given (17) as:

$$C(x,t) = \frac{Co}{\sqrt{4\pi Dt}}\left(\sqrt{\frac{\pi}{2\sqrt{4Dt}}} - \int_0^x e^{-x^2/4Dt}dx\right) \qquad \text{(II-5b)}$$

Assuming a linear relation between the refractive index and the concentration of the solution, an optical path function was written as:

$$Z(x,t) = a\,n(x,t) = a\left[r_o + r_1 C(x,t)\right] \qquad \text{(II-6a)}$$

"a" is the cell thickness in the direction of the optical path. The derivative of Z(x,t) is therefore the Gaussian curve:

$$\frac{\partial Z(x,t)}{\partial x} = \frac{Z_o}{2}\,\frac{1}{\sqrt{4Dt}}\,e^{-x^2/4Dt} \qquad \text{(II-6b)}$$

where $Z = ar_1C_0$.

The measurable path gradient is $\Delta Z/b$, where "b" is the displacement produced by the Savart plate. A given value of $\Delta Z/b$ is represented by a symmetrical fringe pair which separates and then comes back together with diffusion time. The derivative $Z'(x,t)$ was approximated by the measurable path gradient at the neighborhood of the inflection point of the curve when b was small. Therefore:

$$\frac{\Delta Z}{b} = \frac{Z_o}{2} \frac{1}{\sqrt{\pi Dt}} e^{-(x/\sqrt{4Dt})^2} \qquad \text{(II-7)}$$

The movement of a given fringe pair with time was measured and from a suitable relationship between the distance across the fringe pair, $2x$, and time, t, D was calculated from Equation (II-7).

Since in actual experiments an infinitely sharp initial boundary (i.e., step concentration gradient) is not attained, the observed diffusion time was corrected to the hypothetical zero point by a small constant time increment, Δt.

Bryngdahl (8) adopted an iterative procedure for calculating D and Δt from the equation:

$$D = \frac{(2x)^2 \left(\frac{1}{t_1+\Delta t} - \frac{1}{t_2+\Delta t}\right)}{8 \ln \left(\frac{t_2+\Delta t}{t_1+\Delta t}\right)} \qquad \text{(II-8)}$$

D is plotted against $(2x)^2$ for different values of Δt. At the correct value of Δt, a constant D is obtained.

The separation between a selected fringe pair, 2x, was measured by constructing photograms. The next to the outermost fringe pair was used. Diffusion values calculated in a similar manner, using other fringe pairs were reported to agree within .02% (8).

Bryngdahl measured the diffusion coefficients of sucrose using concentration differences as low as 1 gm/100gm water. The precision of the measurements were reported to be within $\pm$0.2%. With a better temperature control for the diffusing system, Bryngdahl stated that the precision of the measurements may approach $\pm$0.1%. The diffusion coefficients obtained for sucrose at 25°C. deviate by about 0.5% from values measured by other authors (8).

Thomas and Nicholl (76) used the single Savart plate birefringent interferometer to determine diffusion coefficients for some electrolytes in water. The optical system was contained in a thermostatically controlled darkroom. The photometric method was also used to gather 2x date. A linear curve fit to the equation:

$$(2x)^2 = 8D(t+\Delta t)\left(1+\ln\frac{t_i+\Delta t}{t+\Delta t}\right) \qquad \text{(II-9)}$$

was used to calculate the values D, Δt and t_i. T_i is the time corresponding to maximum separation between the fringes.

In their study, Thomas and Nicholl (76) reported diffusion coefficients for sucrose in agreement with the precision obtained by Bryngdahl (± 0.2%). For the system monoethanol amine-water, diethanolamine-water, the reproducibilities were up to ± 1%.

Bryngdahl (10) has not reported actual diffusion measurements using the two Savart plate variation of the birefringent interferometer. The principle was adopted by Merliss (46) in his diffusion measurements for glycol in water. Using a calculation procedure adapted to the actual concentration gradient plot obtainable from the experiment, the precision of the measured diffusion coefficients were to ± 2%. The 2x data were taken by direct measurement of the enlarged photograph of the fringe pattern.

Theories of Diffusion Pertinent to the Study

There is at present a large number of published literature on the subject of diffusion in non-electrolyte liquids (58, 78). Though most of the studies were for binary systems, current efforts are directed to the extension of binary theories and models for multicomponent systems. Of particular interest in this study, are experimental and theoretical works on multicomponent systems where the gradient for diffusion is restricted to only one specie. These studies have relied primarily on already existing models for binary and multicomponents systems. This review

will therefore include a discussion of some selected diffusion studies in binary and multicomponent systems.

The existing diffusion theories for binary systems have been derived along four main approaches, namely, via a hydrodynamic approach, from irreversible thermodynamics, from statistical mechanical principles and the theory of rate processes.

The basis for the hydrodynamic theories was independently developed by Einstein and Sutherland (6). From a force balance between the driving force for diffusion and a resistance to flow, the equation for diffusivity was given as:

$$\mathscr{D}_{12} = \frac{kT}{\zeta} \qquad \text{(II-10)}$$

where ζ is a flow resistance term.

Using a rigid sphere model, moving in creeping flow through a continuum, two limiting values for ζ were obtained (6).

$$\zeta = 6\pi\mu_2\mu_1 \qquad r_1 \gg r_2 \qquad \text{(II-11)}$$

$$\zeta = 4\pi\mu_2\mu_1 \qquad r_1 \approx r_2 \qquad \text{(II-12)}$$

Equation (II-10) using ζ evaluated from Equation (II-11) has been shown to provide satisfactory estimates of the diffusivity of dilute solutions of large spherical solutes. The numerical coefficient, 4, from Equation

(II-12) is used in expressions for self-diffusion. Further progress along the hydrodynamic approach required a deeper analysis of the flow resistance coefficient ζ.

Hartley and Crank (31) extended the theory to concentrated solutions by using the gradient of the chemical potential as the driving force for diffusion and by taking into account the motion of both solute and solvent. The resulting equation for diffusion is as follows:

$$\mathcal{D}_{12} = \frac{RT}{N_{av}} \left(\frac{d\ln a_1}{d\ln x_1}\right)\left(\frac{x_1}{\alpha_2 \mu} + \frac{x_2}{\alpha_1 \mu}\right) \qquad \text{(II-13)}$$

The resistance coefficient ζ had been separated into a product of the viscosity and a parameter α with a dimension of length. The usefulness of the equation depends on the correct evaluation of α.

Carman and Stein (15), found that α_1, and α_2 are independent of composition for some solutions. For this condition, α_1 and α_2 were determined from the diffusivities at the two limits of concentration, $\mathcal{D}^\circ_1$ and $\mathcal{D}^\circ_2$. The following linear relationship was obtained:

$$\mathcal{D}_{12}\mu_{12} = \left(\frac{d\ln a_1}{d\ln x_1}\right)\left(x_1 \mu_1 \mathcal{D}^\circ_1 + x_2 \mu_2 \mathcal{D}^\circ_2\right) \qquad \text{(II-14)}$$

The concentration dependence of α_1 and α_2 was considered by Sandquist and Lyons (63) in an empirical manner. They showed that for solutions of diphenyl in benzene the quantity

$$\left[\mathcal{D}_{12} / \frac{d\ln a_1}{d\ln x_1}\right] \frac{\mu_{12}}{\mu_2}$$

is a linear function of the relative viscosity

$$\frac{\mu_{12}-\mu_2}{\mu_{12}}$$

Therefore:

$$\left(\mathcal{D}_{12} \Big/ \frac{d\ln a_1}{d\ln x_1}\right) \frac{\mu_{12}}{\mu_2} = \mathcal{D}_2 + k_2 \frac{\mu_{12}-\mu_2}{\mu_{12}} \qquad \text{(II-15)}$$

and

$$\frac{1}{\alpha_1} = \frac{N_{av}}{RT}\left(\mathcal{D}_2 + k_2 \frac{\mu_{12}-\mu_2}{\mu_1}\right)\mu_2 \qquad \text{(II-16)}$$

where k_2 is the slope of the line described by Equation (II-15). A similar equation may be written for α_2.

Because of the macroscopic nature of the hydrodynamic approach, it fails to provide a general basis for the calculation of the resistance coefficient. A molecular insight to ζ is available through the statistical mechanical approach (4).

The thermodynamic approach developed by Prigogine (52), de Groot (29), Laity (40) and Dunlop (23), do not provide predictive equations for diffusion. However, this approach led to the phenomenological equations of transport, which formed the basis of current developments in diffusional theories.

As previously noted, the problem of the diffusion theory along the hydrodynamic approach had been reduced to the evaluation of the resistance coefficient to diffusion. The statistical mechanical approach, although developed along an entirely different route (4), attempts to provide a molecular basis for the calculation of the friction coefficient.

The frictional coefficient ζ was introduced via the phenomenological equations of transport:

$$\frac{du_1}{dx} = -C_2 \zeta_{12} (v_1 - v_2) \qquad \text{(II-17)}$$

$$\frac{du_2}{dx} = -C_1 \zeta_{12} (v_2 - v_1) \qquad \text{(II-18)}$$

The diffusion coefficient, defined with respect to a volume average velocity, was derived from Equations (II-17) and (II-18) as:

$$\mathcal{D}_{12} = \frac{\bar{V}_2 kT}{\zeta_{12}} \left(1 + \frac{\partial \ln \gamma_1}{\partial \ln c_1} \right) \qquad \text{(II-19)}$$

$$= \frac{\bar{V}_1 kT}{\zeta_{12}} \left(1 + \frac{\partial \ln \gamma_2}{\partial \ln c_2} \right)$$

The frictional coefficient ζ_{12} must be evaluated from an expression involving the potential of intermolecular forces and the radial distribution functions for the molecules. The success of the theory depends on the availability of models to characterize intermolecular forces. Bearman (4) showed that the equations of Eyring (28), Hartley and Crank (31) and Gordon (61) for the concentration dependence of the diffusion coefficients are all equivalent and can be derived from the statistical mechanical theory based on the model of a regular solution.

The rate theory approach provides a kinetic model for the diffusion process. The basic approach was developed by Eyring (28). The liquid was assumed as having a lattice structure with a certain number of "holes." Under the influence of a gradient of chemical potential, a molecule

"jumps" from its initial site to a previously vacant lattice site of distance λ. The frequency of the jumps was given by a rate constant k'. For ideal solutions, where the rate constant k' is identical for both forward and reverse jumps, the resulting equation for diffusion is:

$$\mathcal{D}_{12} = \lambda^2 k' \qquad \text{(II-20)}$$

The rate constant was calculated from the theory of rate processes (28), which states that the desired step is attained through an intermediate activated state. The final form of the diffusion equation was given as:

$$\mathcal{D}_{12} = \frac{\lambda^2}{V_f^{1/3}} \left(\frac{kT}{2\pi m}\right)^{1/2} e^{-\epsilon_o/RT} \qquad \text{(II-21)}$$

where

ϵ_o = activation energy per molecule at 0°K.

V_f = free volume, i.e., volume available for each molecule

$\lambda = \left(V/Nav\right)^{1/3}$

m = mass of the molecule

V = molar volume

Nav = Avogadros number

An equation similar to that obtained from hydrodynamic theories was derived by assuming that the process of diffusion is comparable with that for viscous flow (28). The treatment is applicable for the self diffusion of pure components. When two types of molecules are involved, as in binary diffusion, it was pointed out that mean values of λ, heat of vaporiztion, ΔEvap, and the reduced mass of solute and solvent, may be used. (28)

A correction for the inequality of the free energies of the initial and final states was used for concentrated solutions to arrive at the following form:

$$\mathcal{D}_{12} = \mathcal{D}^{\circ}_{12} \frac{d\ln a_1}{d\ln x_1} \qquad \text{(II-22)}$$

Equations (II-21) and (II-22) have been found to give only order of magnitude agreement with experimental data. Olander (51) and Gainer and Metzner (27) later pointed out the inadequacy of the simple lattice model consisting of only one type of molecule to describe binary systems.

A modification of the absolute rate theory, to account for the presence of two types of molecules in binary diffusion, was proposed by Olander (51). For the group

$$\frac{\mathcal{D}_{12}\mu_{12}}{T}$$

a distinction was made between the free energies of activation for the viscous and diffusive processes. The resulting equation is:

$$Y = \left(\frac{\Omega_{12}\mu_{12}}{T}\right)\left(\frac{\xi}{k}\right)\left(\frac{V}{N_{av}}\right)^{1/3} = \exp\left\{\frac{\Delta G_{\mu}-\Delta G_{D}}{RT}\right\} \quad \text{(II-23)}$$

where

ξ = 5.6 using Eyring's value (51)

ΔG_{μ} = total activation energy for viscous flow

ΔG_{D} = total activation energy for diffusion

The processes, both for viscous flow and diffusion, are pictured in two stages: the formation of a hole or vacant lattice site followed by the movement of a neighboring molecule into the vacated site. For viscous flow both steps involve interaction between identical species. In diffusion, the second step involves solute-solvent interaction. Therefore:

$$\Delta G_{u} = \Delta G^{h}_{AA} + \Delta G^{j}_{AA} \quad \text{(II-24)}$$

$$\Delta G_{D} = \Delta G^{h}_{AA} + \Delta G^{j}_{AS}$$

The activation energy term in Equation (II-20) reduces to:

$$\exp\left(\frac{\Delta G_{u}-\Delta G_{D}}{RT}\right) = \exp\left(\frac{\Delta G^{j}_{AA} - \Delta G^{j}_{AS}}{RT}\right) \quad \text{(II-25)}$$

Approximations were made to characterize the molecular interactions and the free energy term was estimated as:

$$\frac{\Delta G^{j}_{AA} - \Delta G^{j}_{AS}}{RT} = f\delta \qquad \text{(II-26)}$$

where "f" is the fraction of the total free energy of activation due to the bond breaking step and δ was given by the expression:

$$\delta = \frac{\Delta G_{AA}}{RT}\left(1 - \frac{\Delta G_{SS}}{\Delta G_{AA}}\right)^{1/2} \qquad \text{(II-27)}$$

The term "f" was empirically determined from several binary systems to be $\frac{1}{2}$. The activation energies to be used in Equation (II-24) maybe calculated from:

$$\frac{\Delta G}{RT} = \ln\left[\frac{\mu V}{hN_{av}}\right] \qquad \text{(II-28)}$$

Cullinan (18) used the Eyring absolute rate theory to explain the remarkably good agreement of a large number of binary diffusion experimental data to an empirical equation presented by Vignes (80).

The net motion between the solute and solvent molecules was described as an over-all process taking place via an activated configuration.

Therefore:

$$(v_2 - v_1) = \frac{\lambda^2}{hN_{av}X_2} e^{-\Delta G_{12}/RT} \Delta u_1 \qquad \text{(II-29)}$$

The driving force for diffusion was related to the friction coefficient via the phenomenological relation (4):

$$\Delta u_1 = F_{12}C_2(V_2-V_1) \qquad \text{(II-30)}$$

Equation (II-26) becomes:

$$F_{12} = \frac{hN_{av}}{C\lambda^2} e^{\Delta G_{12}/RT} \qquad \text{(II-31)}$$

The concentration dependence of the friction coefficient was expressed by assuming a mixing rule for the total activation energy:

$$\Delta G_{12} = X_1\Delta G^{\circ}_{21} + X_2\Delta G^{\circ}_{12} \qquad \text{(II-32)}$$

The values ΔG°_{21} and ΔG°_{12} are values at the composition extremes and are related to the corresponding friction coefficients as follows:

$$F^{\circ}_{12} = \frac{hN_{av}}{C_1\lambda^2} e^{\Delta G^{\circ}_{12}/RT} \qquad \text{(II-33)}$$

$$F^{\circ}_{21} = \frac{hN_{av}}{C_2\lambda^2} e^{\Delta G^{\circ}_{21}/RT} \qquad \text{(II-34)}$$

The diffusion coefficient defined with respect to the volume average velocity is related to Equation (II-31) by the expression:

$$F_{12} = \frac{RT}{\vartheta_{12}C}\left(1 + \frac{d\ln \gamma_1}{d\ln x_1}\right) \qquad \text{(II-35)}$$

Substituting Equations (II-31) to (II-34) and using the defining Equation (II-35), the final form of the equation is, as derived earlier by Vignes (80):

$$\mathcal{D}_{12} = (\mathcal{D}_{12}^{\circ})^{x_2} (\mathcal{D}_{21}^{\circ})^{x_1} \left(1 + \frac{d\ln a_1}{d\ln x_1}\right) \quad \text{(II-36)}$$

Comparatively little work has been done for multicomponent systems. This is due in a large part to the lack of a rigorous theory for the liquid state. To date, only two contributions have dealt with a predictive method for estimating multicomponent diffusion coefficients.

Lightfoot et. al. (43), using the phenomenological theory of transport, obtained a generalized equation similar to the Stefan-Maxwell equation for gases. The equation is however, useful only as a first approximation for predicting liquid multicomponent diffusion coefficients.

The Vignes-Cullinan equation for binary diffusion (18, 80) had been extended to multicomponent systems (20). It must be noted, however, that despite the apparent connection of the former with the absolute rate theory, the equations were developed from an empirical basis and give no real kinetic insight into the diffusion process.

The friction coefficients were expressed in terms of the values of the friction coefficients at the composition extremes as follows:

$$F_{ij} = \frac{1}{C} \frac{L}{\prod_k} (\lim_{X_K \to 1} CF_{ij})^{X_K} \quad \text{(II-37)}$$

Equation (II-37) is a direct result of the assumption of a linear mixing rule for the total activation energy. At the composition extremes the friction coefficients were expressed in terms of binary diffusion coefficients by the following equations:

$$\lim_{X_i \to 1} F_{ij} = \frac{RTV_i}{\mathcal{D}^{\circ}_{ji}} \qquad \text{(II-38)}$$

$$\lim_{X_j \to 1} F_{ij} = \frac{RTV_j}{\mathcal{D}^{\circ}_{ij}} \qquad \text{(II-39)}$$

$$\lim_{X_K \to 1} F_{ij} = \frac{1}{\mathcal{D}^{\circ}_{ik}\mathcal{D}^{\circ}_{jK}} \lim RT\left(\frac{D^{K}_{ij}}{C_i} - \mathcal{D}^{\circ}_{iK}\, u^{K}_{ij}\right) \qquad \text{(II-40)}$$

D^{K}_{ij} is a multicomponent diffusion coefficient and hence makes the absolute evaluation of F_{ij} impossible. For the case where:

$$\lim_{X_K \to 1} \frac{D^{K}_{ij}}{C_i} \longrightarrow 0 \qquad \text{(II-41)}$$

Equation (II-40) was written as:

$$\lim_{X_K \to 1} F_{ij} = \frac{RTV_K}{\alpha^{K}_{ij}\mathcal{D}^{\circ}_{jK}} \qquad \text{(II-42)}$$

where $$\alpha_{ij}^{K} = \frac{-RTV_K}{\lim u_{ij}^{K}} \qquad \text{(II-43)}$$

The parameter α_{ij}^{K} was evaluated from thermodynamic considerations and symmetry requirements to be:

$$\alpha_{ij}^{K} = \frac{V_K\left(1 - \frac{\mathcal{D}_{iK}^{\circ}}{\mathcal{D}_{jK}^{\circ}}\right)}{(V_i - V_j)} \qquad \text{(II-44)}$$

The final form of Equation (II-37) was given as:

$$F_{ij} = \frac{RT}{C}\left[\prod_{k\neq i,j}^{L}\left(\alpha_{ij}\right)^{X_k}\right]^{-1}\left[\left(\mathcal{D}_{ji}^{\circ}\right)^{X_i}\left(\mathcal{D}_{iJ}\right)^{X_J}\prod_{K\neq i,J}^{L}\left(\mathcal{D}_{JK}^{\circ}\right)^{X_k}\right]^{-1} \qquad \text{(II-45)}$$

The corresponding multicomponent diffusion coefficients are calculated from the inverted forms of the equations of Dunlop (23) expressing the frictional coefficients in terms of the diffusion coefficients.

For several nonassociated ternary systems, Cullinan (20) found that the average absolute deviation between the predicted and experimental values were less than 9%.

It was noted, that for nearly ideal systems all the $\alpha_{ij}^{K} = 1$ and only one diffusion coefficient, D^{*} is needed to describe the system.

$$D^* = (\mathscr{D}^o_{ji})^{x_i} (\mathscr{D}^o_{ij})^{x_j} \prod_{K \neq i,j}^{L} (\mathscr{D}^o_{jK})^{x_k} \qquad \text{(II-46)}$$

The equivalent expression obtained empirically by Burchard and Toor (11), expresed D* as a linear function of the binary diffusivities and the mole fraction.

Due to the simpler, but nevertheless practical nature of the diffusion of a single specie through a mixture of solvents, this particular case of multicomponent diffusion has received separate attention. At the present time, all the available predictive methods are for the diffusion of a dilute liquid component.

All the studies, (36,43,74) except for the work of Cullinan and Cusick are based on the use of an effective binary diffusivity D_{1m}, as first applied in the diffusion of a single gas in a stagnant multicomponent gas mixture. In effect, the system is treated as a pseudobinary, with the solute diffusing through a single component, the properties of which consist of appropriately weighted averages of the solvent components.

For the diffusion of a trace component 1 through a mixture 2 and 3, the multicomponent equations by Lightfoot, et. al. (43), were reduced to the following:

$$\frac{1}{D_{1m}} = \left(\frac{x_2}{\mathscr{D}^o_{12}} + \frac{x_3}{\mathscr{D}^o_{13}} \right) \frac{d\ln x_1}{d\ln a_1} \qquad \text{(II-47)}$$

Discrepancies of up to 30% between the measured and predicted values were found (36).

The diffusion of dilute toluene in two component solvent mixtures of paraffinic hydrocarbons were studied by Holmes et. al. (36). They found that the data, plotted as the group $\frac{D\mu}{T}$ vs. $\bar{M}$, behaved like a binary if the mole fraction average molecular weight of the two components were used for the solvent molecular weight. A linear relationship was found for most of the systems studied. The data were also interpreted in terms of the modified absolute rate theory of Olander (51), using mole fraction averages of the mixed solvents for the parameter δ. The data were 15% higher than the values predicted by the modified absolute rate theory (36).

Tang and Himmelblau (74) used an empirical treatment to evaluate the free energy term in the modified absolute rate theory (51). The theory was reduced to the form:

$$B\left(\frac{D_{lm}\mu_m}{T}^{1/2}\right) V_m^{-1/6} = \exp\left(-\frac{\Delta G_{lm}}{RT}\right) \qquad \text{(II-48)}$$

where:

$$B = \delta/(kh^{1/2}N_{av}^{5/6})$$

Two mixing rules for the total activation energy term were used:

$$\exp\left(-\frac{\Delta G_{1m}}{RT}\right) = X_2 \exp\left(-\frac{\Delta G_{12}}{RT}\right) + X_3 \exp\left(-\frac{\Delta G_{13}}{RT}\right) \quad \text{(II-49)}$$

$$\Delta G_{1m} = x_2 \Delta G_{12} + x_3 \Delta G_{13} \quad \text{(II-50)}$$

The respective resulting predictive equations were given as follows:

$$D_{1m}\mu_m^{1/2}V_m^{-1/6} = x_2 \mathcal{D}_{12}\mu_2^{-1/6} + x_3 \mathcal{D}_{13}\mu_3^{1/2}V_3^{-1/6} \quad \text{(II-51)}$$

$$\log\left(D_{1m}\mu_m^{1/2}\right) = x_2 \log\left(\mathcal{D}_{12}\mu_2^{1/2}\right) + x_3 \log\left(\mathcal{D}_{13}\mu_3^{1/2}\right) \quad \text{(II-52)}$$

No preference over the two equations was cited. Both equations were found to predict to within 10% experimental data for the systems used by Holmes (36), for carbon dioxide-hydrocarbon pairs as well as carbon dioxide-ethanol-water system.

Based on their multicomponent diffusion theory, Cullinan and Cusick (19) developed an equation for the case of the transport of a trace amount of specie 1 through a mixture of 2 and 3.

$$\frac{\lim D_{1n}}{x_1 \to o} = \left[\frac{x_2}{\left(\mathcal{D}^o_{12}\right)^{x_2}\left(\alpha^3_{12}\,\mathcal{D}^o_{23}\right)^{x_3}} + \frac{x_3}{\left(\mathcal{D}^o_{13}\right)^{x_3}\left(\alpha^2_{13}\,\mathcal{D}^o_{32}\right)^{x_2}}\right]^{-1} \quad \text{(II-53)}$$

where

$$\alpha_{ij}^{K} = \frac{V_K\left(1-\frac{\mathcal{D}^{o}_{iK}}{\mathcal{D}_{jK}}\right)}{(V_i-V_j)} \qquad \text{(II-54)}$$

The equations were found to predict successfully the diffusion coefficients for benzene-acetone-carbon tetrachloride and acetone-benzene-carbon tetrachloride system.

The literature review show that there is considerable activity devoted to a theoretical description of diffusion. The statistical mechanical approach seem to indicate the direction where the most general results can be obtained. Further development must however, await advances in the molecular aspects of a liquid theory. From a semi-empirical approach, the works of Cullinan (18,19) seem to provide moderately successful results for the prediction of diffusion coefficients.

CHAPTER III

EXPERIMENTAL APPARATUS

In this study, experimental measurements were made of diffusion coefficients, viscosities and densities of the system uranyl nitrate-tributyl phosphate-n-heptane.

Diffusion Apparatus

The diffusion apparatus consisted of the following: the optical system, the diffusion cell and the constant temperature bath.

The Optical System

The optical system is a modification of one constructed by Skinner (69) and is similar to the one used earlier by Bryngdahl (8). It consists of an optical bench, a light source, three lenses, a Savart plate, a polarizer and a camera. The arrangement is described schematically in Figure 2. A two Savart plate arrangement, a modification of the method later proposed by Bryngdahl (10), was initially attempted in this study, but was not successful. Some details of the procedures used are given in Appendix A.

The light source was a Spectra Physics helium-neon gas laser, Model 130. The laser produces a monochromatic

L - LENS
S - SAVART PLATE
P - POLARIZER

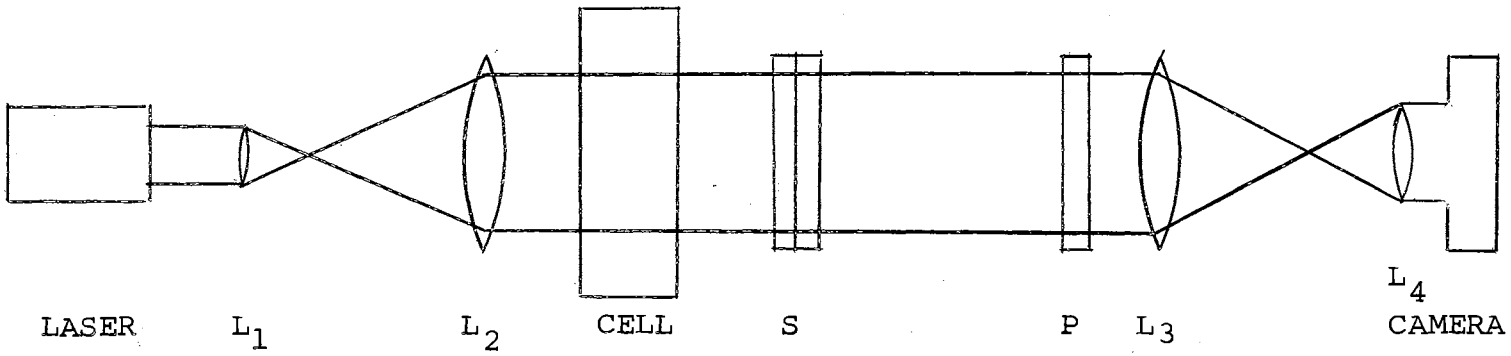

Figure 2. Optical Arrangement of One Savart Plate Interferometer for This Study

6328 Å collimated light beam about 1.5 mm in diameter and 0.005 watts power output. The light beam from the laser was expanded and recollimated by using two lenses: L1, 17mm in diameter with a 12 mm focal length and L2, 56 mm in diameter with a 305 mm focal length.

The Savart plate, S, was placed in the collimated light path next to the diffusion cell. The Savart plate was made of two quartz crystal plates each 10 mm thick and $1\frac{1}{2}$ inches square placed together, with their optical axis at 90° to each other. The Savart plate was rotated to divide the ordinary and extraordinary rays of the light beam in the vertical direction.

The plane polarizer, P, with its electric vector in the horizontal plane was mounted in the same lens mount for L3. L3, a 48 mm. diameter lens with a 343 mm focal length, together with the extended camera lens was used to reduce the size of the cell image.

The resulting fringe pattern was photographed with a 35 mm Nikon Model F camera equipped with a two inch lens extension.

Lenses, L1, L2, L3, are compound lenses corrected for both chromatic and spherical aberrations and were purchased from Edmund Scientific Company. The polarizer, P, and Savart plate, S, were purchased from Karl Lambrecht Crystal Optics.

The optical components were mounted on an optical bench and aligned according to the procedure described by Slater (71).

The Diffusion Cell

The diffusion cell was a flowing junction type. It was a modification of the interfacial turbulence cell used by Skinner (69). A sectional view of the diffusion cell is Shown in Figure 3. The cell was constructed at the Research and Development Laboratory, Oklahoma State University.

The cell was constructed of four stainless steel plates pinned to a brass frame to form a rectangular cell open along two verical walls. The two other walls perpendicular to the light path were made of glass optical flats. The solution chamber was $\frac{1}{4}$ inch wide, two inches deep (along the optical path) and three inches high. The chamber had a funnel shaped top and bottom to prevent the trapping of air. The cell had two openings, each one $\frac{1}{8}$ inch in diameter, in both the top and the bottom. It had also two openings at the center of the two stainless steel sides, each a 0.006 inch inch slit, 2 inches long. All the openings were fitted with stainless steel Swagelock fittings. The solution tanks were one liter glass separatory funnels. The feed and discharge lines were made from $\frac{1}{4}$ inch Teflon tubing. Flow was controlled with $\frac{1}{16}$ inch stainless steel needle valves. The cell had a three point adjustable mount to allow alignment with the optical system.

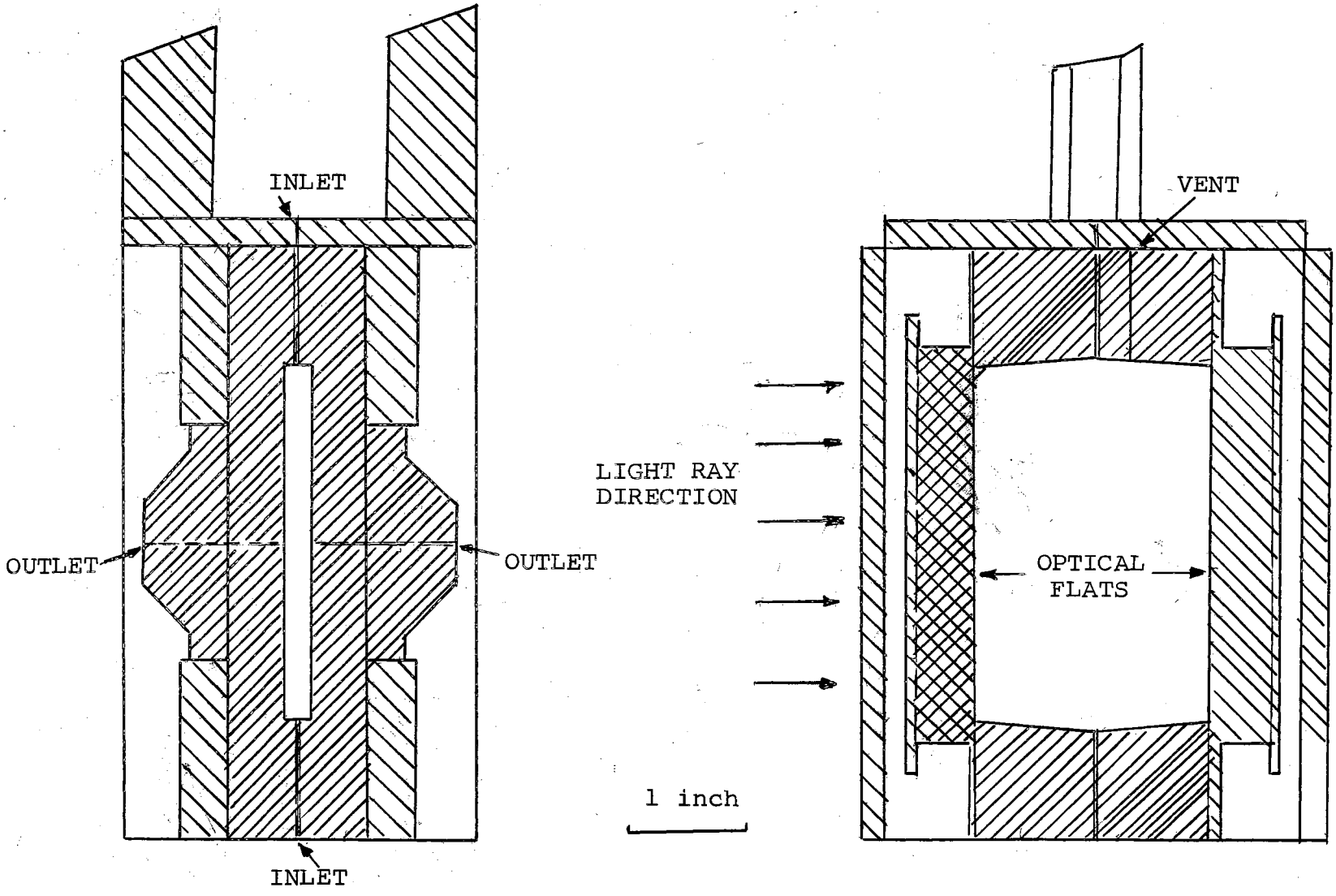

Figure 3. Flowing Junction Diffusion Cell

Constant Temperature Bath

The diffusion cell was immersed in a constant temperature water bath which was mounted directly to the optical bench. The constant temperature bath was the same one used by Skinner (69).

Auxiliary Apparatus

Solution density data were taken by multiple weighing of a 25 ml. volumetric flask using a Mettler analytical balance.

Solution viscosities were determined by using two Cross Arm Viscometers, Model C-50.

A Beckman DU Spectrophotometer was used in the analytical determination of uranium.

Measurements from the recorded fringe patterns were made in a Vanguard Motion Analyzer with readings of .001 inch increment on image.

Materials

The commercial grade tributyl phosphate was purchased from Commercial Solvents Corporation. The tributyl phosphate was purified by boiling one liter of tributyl phosphate with one-half liter of 0.5N NaOH at total reflux for ten hours. The mixture was further allowed to boil without reflux for one hour. The mixture was poured into a three liter separatory funnel and the aqueous NaOH solution was decanted. The remaining tributyl phosphate was washed

repeatedly with distilled water until neutral, as shown by litmus paper.

The n-heptane used was pure grade, purchased from Phillips Petroleum Co. The n-heptane was used as received.

The uranyl nitrate used in this work was recrystallized from aqueous uranyl nitrate solutions. The water from the aqueous solution were evaporated by using two infrared lamps placed three feet above the tray containing the solution. The purity of the recovered uranium was analyzed by comparing the refractive index of a sample whose concentration has been determined spectrophotometrically, with a corresponding solution prepared using ACS reagent grade uranyl nitrate. The original uranyl nitrate was purchased from the General Chemical Division of Allied Chemical Company.

The NaCl used for the standard diffusion experiment was certified ACS grade purchased from Fisher Scientific Company.

Photographs were taken using a high contrast film, Kodak High Contrast Copy M417. The films were developed in Baumann Diafine Two Bath Film Developer.

CHAPTER IV

EXPERIMENTAL PROCEDURE

The procedures followed to obtain the experimental diffusion coefficients, densities and viscosities are given in the following paragraphs.

Preparation of Solutions

The aqueous NaCl solutions used in the standard diffusion experiment were prepared by weighing the salt on an analytical balance and dissolving in appropriate volumes of distilled water.

The tributyl phosphate-n-heptane mixtures were prepared in one liter batches. The desired amount of tributyl phosphate was pipeted into a one liter volumetric flask. The n-heptane was added until the one liter mark was reached. The water emulsion that was formed was broken by filtering the solution.

The tributyl phosphate-n-heptane mixture was saturated with uranyl nitrate hexahydrate crystals at room temperature. More salt was added and the mixture was allowed to stand for 24 hours, being shaken regularly. The resulting aqueous layer was separated from the organic layer in a separatory funnel.

The uranyl nitrate concentration of the resulting organic solution was analyzed by the potassium ferrocyanide method of Dizdar and Obernovic (22). The step by step procedure is given by Slater (70). The analysis takes place after extraction of the uranyl nitrate from the organic to an aqueous phase. The extractions involve very dilute solutions of uranyl nitrate, and in this region, 99% of the solute is extracted. The saturated uranyl nitrate solution for a given tributyl phosphate-n-heptane mixture served as the stock solution from which all other solutions were prepared by careful dilution.

To obtain the solution for 0.02 M uranyl nitrate-TBP complex in pure n-heptane (Run #0A), a saturated solution of uranyl nitrate in 30 V/V % TBP-n-heptane was diluted with the necessary volume of n-heptane.

The Diffusion Runs

To obtain the necessary data for the calculation of diffusion coefficients, the following steps were followed: (1) the diffusion cell was cleaned and mounted in the constant temperature water bath, (2) the cell was filled with liquid and the flow adjusted to obtain a sharp interface, (3) the solution was brought to a constant temperature, (4) photographs of the fringe patterns were taken at different time intervals and (5) measurements were taken from the photographs using the Vanguard Motion Analyzer.

First, the temperature control system was started, the temperature in the water bath was controlled to 25.00 $\pm$ 0.005°C.

The diffusion cell was cleaned by first washing with acetone. Then the cell was repeatedly rinsed with distilled water. The cell was carefully placed in an ultrasonic cleaner filled with distilled water and left for about 30 minutes. This procedure cleaned the slit of all dirt not removed by a water jet. The cell was finally rinsed with distilled water and blown dry with dried air. The optical flats were cleaned with ethyl alcohol and rinsed with distilled water. The surfaces were then dried and polished with Kimwipes. The teflon gaskets were cleaned in a similar manner. The optical flats were affixed to the cell, between the teflon gasket and a brass plate, by applying uniform pressure around the edges of the flat. The feed tanks and the flow lines were cleaned by passing acetone, rinsing with distilled water and drying with dry air. The cell was then mounted in the constant temperature water bath.

The flow lines were clamped tight to the corresponding cell openings and the valves closed. The feed tank for the more dense liquid was filled. The stop cock of the feed tank with the denser liquid was opened and the more dense solution was allowed to fill the cell chamber to the base of the feed tank for the less dense liquid. By this procedure, air bubbles in the cell and feed lines were removed.

Then the stopcock to the feed tank for the less dense liquid was opened. The solution was allowed to fill the two discharge flow lines by opening the discharge valves. When all the air bubbles in the cell and the flow lines were removed, all the valves and stopcocks were closed. The feed tank for the less dense solution was filled and the stopcocks to the feed tanks were opened. The discharge valves were opened to maintain a small liquid flow.

At this point the laser beam was turned on to observe the cell image in the camera.

After about two to three hours, when the interface between the solutions in the diffusion cell started to form, the discharge flow rate was decreased and adjusted. A flow rate of 30 drops per minute was maintained for at least thirty minutes or until a sharp interface was established.

The camera was moved along the optical bench until a very sharp dark line was observed at the center of the cell image. A photograph was taken and labeled as interface, or uncorrected zero time.

The temperature control system was turned off to prevent any vibration to be transmitted to the diffusing system and the temperature was recorded.

The discharge valves were turned off immediately and the clock simultaneously turned on. The stopcocks of the feed tanks were closed to prevent any movement of the interface. Photographs were taken at suitable intervals

of the run such that thirty-six exposures were taken for each run. An exposure time of one-fifteenth of a second produced the desired contrast in the film.

After one run was completed, that is, when the next to the outermost fringe pair had come together, the temperature was recorded. The temperature control was turned on and the water bath was brought to constant temperature. The interface was resharpened and another run was made. For a given solution three consecutive runs were made.

When three runs had been completed for a given solution, the feed tanks and the cell was emptied. The solution was passed through an opening at the bottom of the cell, at this time connected to the discharge flow line. The cell and the flow lines were emptied completely. The cell was then rinsed with the new solution to be studied.

At the end of a series of runs for a given tributyl phosphate-n-heptane dilution, the cell was removed and cleaned.

The films were developed in a two bath Diafine developer and allowed to dry.

The movement of the next to the outermost fringe pair was examined in the Vanguard motion analyzer, which magnifies the photographs about seventeen times. The distance between the centers of the fringe pair were measured and recorded as "$2x$" measurement for each photograph. Two to three readings were made each time. The

$2x$ and time data for a given run were used to calculate diffusion coefficients for that run.

The proper location of the camera, in order to obtain symmetrical fringe pairs was determined using the NaCl solution. A detailed procedure was given by Slater (71). Diffusion runs were taken at different locations of the camera, along the optical bench, to include points behind and in front of the proper position. The separation between the first two fringes on both sides of the center of the fringe pattern, after one minute of uncorrected diffusion time, was measured. The camera position was established at the point where the ratio of the distances equal one.

It was found by trial and error that a concentration gradient of .02 M uranyl nitrate provided the optimum balance of refractive index gradient, i.e., the number of fringe pairs, and the density gradient for a stable interface.

Density and Viscosity Measurements

Solution densities were taken by weighing the liquid in a 25 ml. volumetric flask calibrated with water. The solutions were first brought to constant termperature for about two hours, in a water bath kept at $25.0 \pm .01°C$. The solutions were quickly transferred to the 25 ml. volumetric flask by means of a pipette. The liquid level was adjusted to the mark by a dropper. The flask was covered and wiped dry by Kimwipes. The flask and solution was then

weighed in a Mettler balance. Two determinations were made for each solution.

Solution viscosities were measured using two Cross Arm viscometers. Each viscometer was filled to the mark with the sample and placed in the constant temperature water bath for ten minutes. A suction was applied and the liquid flow time was recorded. The viscometers were calibrated with water by the standard technique.

CHAPTER V

EXPERIMENTAL RESULTS

Differential diffusion coefficients at 25°C were obtained for the following systems: uranyl nitrate in 30 V/V percent tributyl phosphate-n-heptane, uranyl nitrate in 50 V/V percent tributyl phosphate-n-heptane, uranyl nitrate in 70 V/V percent tributyl phosphate-n-heptane and for .01 M uranyl nitrate in TBP and in pure n-heptane. At 30 V/V percent, 50 V/V percent and 70 V/V percent TBP-n-heptane, the entire concentration range up to saturation with respect to uranyl nitrate was covered. Density and viscosity measurements at 25°C were also taken.

Calculation of Diffusion Coefficients from Experimental Data

In this study, the diffusion runs were recorded photographically. Figure 4 presents photographs of the center of the cell chamber taken at various times during the diffusion run for Run 7D1. They show: the initial interface just before diffusion is started designated $t = 0$, the fringe pattern at times $t = 210$ and 510 seconds, and near the end of diffusion $t = 1,620$ seconds.

The experimental data consist of measurements, taken

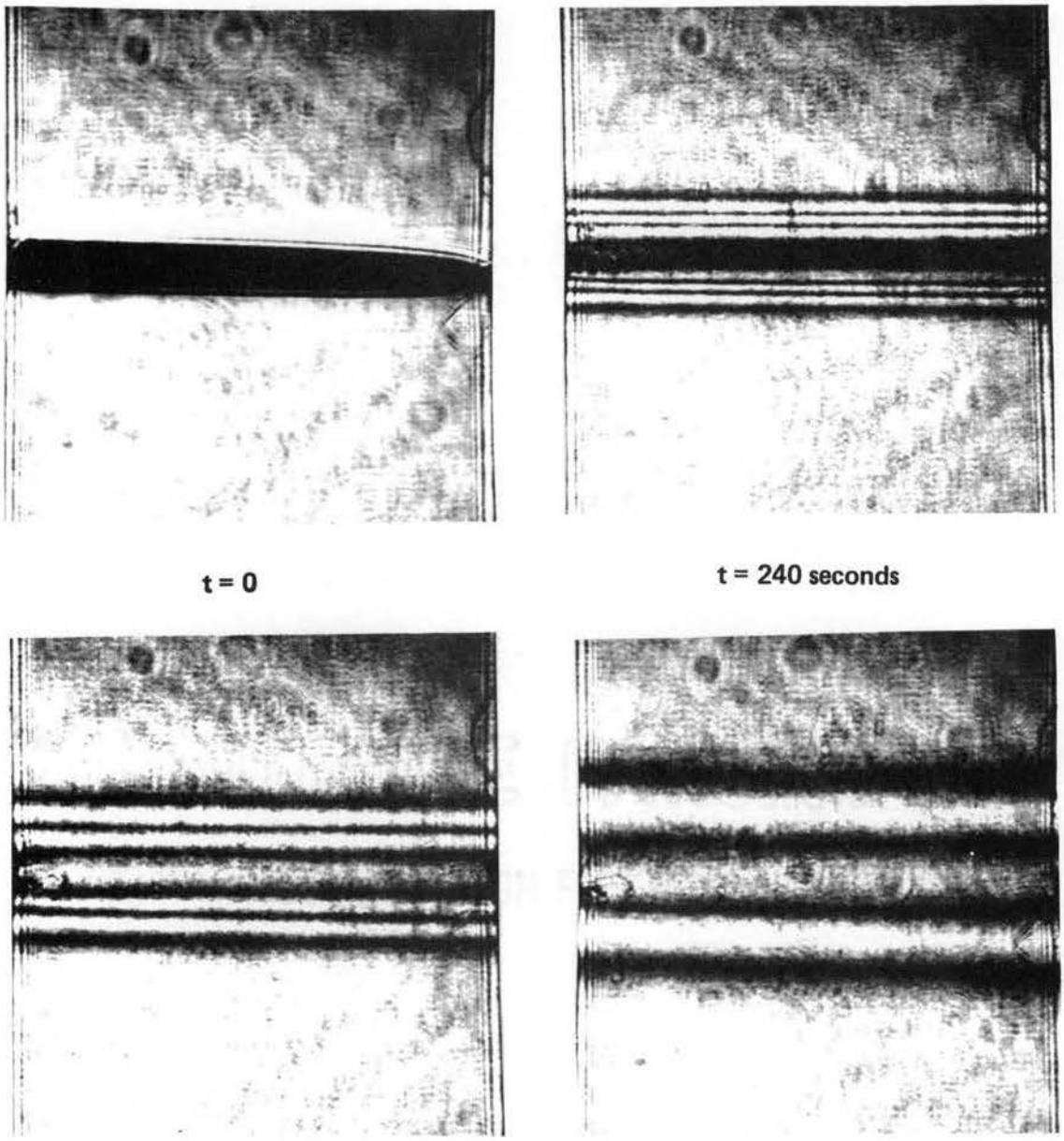

Figure 4. Photographs of Diffusion Run (Run 7D1)

from the photographs, of the separation distance between the next to the outermost fringe pair, $2\bar{x}$, and the recorded time, t. A plot of the data, presented as $(2\bar{x})^2$ against time, t, is shown in Figure 5.

Bryngdahl (8) has shown that a plot of $(2\bar{x})^2$ against t, starting from an infinitely sharp interface can be represented by the equation:

$$(2\bar{x})^2 = 8 \cdot Dt\left(1 + \ln\frac{t_i}{t}\right) \qquad (V\text{-}1)$$

where t_i correspond to the time of maximum separation between the fringes.

In actual diffusion measurements, an infinitely sharp interface is never attained, a correction for a finite interface in the form of a time correction, Δt, is included in Equation (V-1) (8). Fujita (26) has in fact shown that Δt may be calculated from the dimensions of the finite interface. The equation used was therefore (8):

$$(2x)^2 \cdot MF = 8 \cdot D \cdot (t+\Delta t)\left(1+\ln\frac{t_i+\Delta t}{t+\Delta t}\right) \qquad (V\text{-}2)$$

A non-linear regression program obtained from Erbar (24) was used to evaluate the constants D, Δt, and t_i as parameters corresponding to the best fit of the data to Equation (V-2). The program is based on the non-linear curve fitting method devised by Marquardt (44), which is a combination of the Gauss-Newton and Steepest Ascent procedures. The complete $(2x)^2$ and t data were used except for some points near the end of the run, in order to obtain

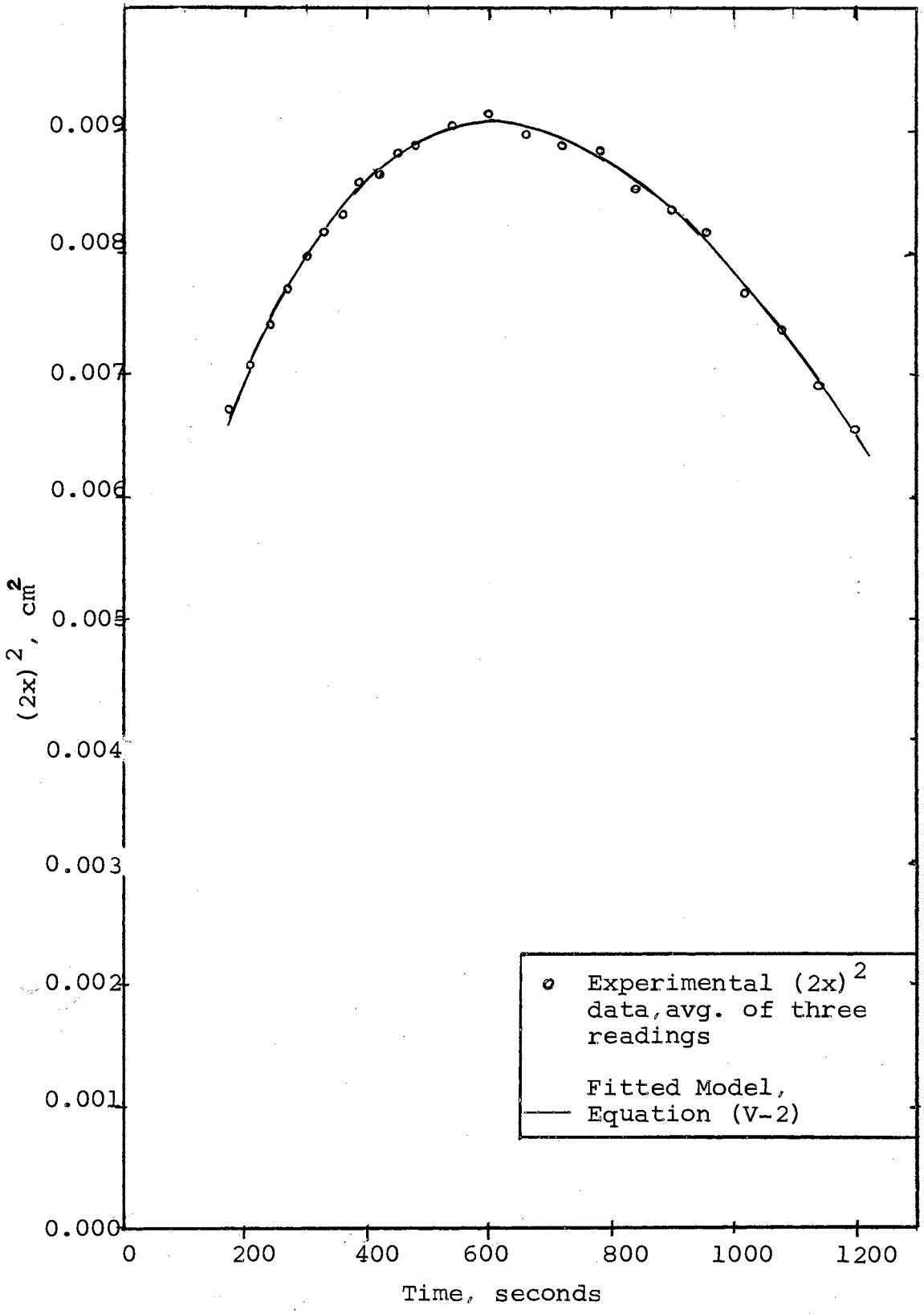

Figure 5. Plot of Experimental Fringe Measurement and Equation (V-2)

an experimental curve that is equally weighted on both sides of its peak.

The value of the magnification factor MF, was determined from a diffusion run using aqueous NaCl solution. The (2x) vs. time data were fitted to Equation (V-2) with D set at the literature value of 1.474×10^{-5} (59) for 0.25M NaCl at 25°C. Table I presents the results of three runs. The magnification factor was also independently determined from measured dimensions of the cell cavity and the corresponding image recorded in the photographs, to be .004678. The average value of the magnification factor determined from NaCl is checked to within $\pm$ 1.4%.

Figure 5 also shows a comparison of the experimentally measured data and the curve as determined from Equation (V-2). An analysis of the errors introduced in the determination of the diffusion coefficients is presented in Chapter VI.

Diffusion Data for the System Uranyl Nitrate-Tributyl Phosphate-n-Heptane

A tabulation of the calculated values of D, Δt and t_i for all the systems studied are presented in Tables II, III, IV, V, and VI. Each run number indicated by the same first number and letter refer to diffusion runs made from the same solution and the last number refers to whether the run was the first, second or the third one made. The letter indicate the chronological order in which the

TABLE I

MAGNIFICATION FACTOR USING
STANDARD NaCl SOLUTION *

Run No.	ΔC mole/l	$\bar{C}$ mole/l	t_i sec	Δt sec	MF	$(MF)_{ave}$
511	.094	0.25	300	21	.004609	
512	.094	0.25	297	23	.004622	.004614
513	.094	0.25	298	23	.004610	

$^{*}D = 1.474 \times 10^{-5}$ cm^2/sec (59)

TABLE II

DIFFUSION COEFFICIENTS AT 25°C FOR THE SYSTEM URANYL NITRATE IN 30 V/V % TRIBUTYL PHOSPHATE - 70 V/V % N HEPTANE

Run No.	ΔC_{UN} moles/l	$\bar{C}_{UN}$ moles/l	t_i sec	Δt sec	$D \times 10^6$ cm^2/sec	$(\bar{D} \pm \Delta D) \times 10^6$ cm^2/sec
3A1	0.017	0.481	87	37	3.383	
3A2	0.017	0.481	81	51	3.378	3.381±.003
3A3	0.017	0.481	92	42	3.382	
3B2	0.018	0.401	206	56	3.561	3.616±.055
3B3	0.018	0.401	210	49	3.671	
3C1	0.020	0.300	249	46	3.727	
3C2	0.020	0.300	248	43	3.775	3.771±.029
3C3	0.020	0.300	243	44	3.811	
3D1	0.019	0.200	200	43	4.173	4.179±.005
3D2	0.019	0.200	212	36	4.184	
3E1	0.020	0.100	197	36	4.079	
3E2	0.020	0.100	209	46	3.964	3.994±.057
3E3	0.020	0.100	224	42	3.938	
3F1	0.020	0.050	279	67	3.797	
3F2	0.020	0.050	278	72	3.784	3.791±.005
3F3	0.020	0.050	287	65	3.793	
3G2	0.020	0.010	303	69	3.910	3.956±.046
3G3	0.020	0.010	301	66	4.002	
3P2	0.018	0.030	195	51	3.482	3.675±.193
3P3	0.018	0.030	192	48	3.869	
3I4	0.020	0.150	422	97	3.661	3.601±.060
3I5	0.020	0.150	457	105	3.540	

TABLE III

DIFFUSION COEFFICIENTS AT 25°C FOR THE SYSTEM URANYL NITRATE IN 50 V/V % TRIBUTYL PHOSPHATE - 50 V/V % N HEPTANE

Run No.	ΔC_{UN} moles/l	$\bar{C}_{UN}$ moles/l	t_i sec	Δt sec	$D \times 10^6$ cm^2/sec	$(\bar{D} \pm \Delta D) \times 10^6$ cm^2/sec
5A3	0.020	0.341	558	82	2.720	2.833±.113
5A4	0.020	0.341	549	63	2.946	
5B2	0.019	0.200	262	59	2.505	2.431±.074
5B3	0.019	0.200	264	70	2.357	
5C2	0.020	0.100	663	137	2.516	2.485±.031
5C3	0.020	0.100	660	147	2.454	
5D1	0.020	0.050	318	67	2.797	2.772±.021
5D3	0.020	0.050	358	69	2.751	
5E1	0.020	0.010	1277	276	3.175	3.050±.122
5E3	0.020	0.010	1430	373	2.931	
5F2	0.020	0.900	368	114	2.039	2.015±.024
5F3	0.020	0.900	384	98	1.988	
5G2	0.020	0.750	482	55	2.210	2.199±.011
5G3	0.020	0.750	543	76	2.188	
5H2	0.018	0.500	100	79	1.880	1.873±.007
5H3	0.018	0.500	100	77	1.866	
5I2	0.020	0.350	394	84	2.342	2.342±.0005
5I3	0.020	0.350	408	97	2.343	

TABLE IV

DIFFUSION COEFFICIENTS AT 25°C FOR THE SYSTEM URANYL NITRATE IN 70 V/V % TRIBUTYL PHOSPHATE - 30 V/V % N HEPTANE

Run No.	ΔC_{UN} moles/l	$\bar{C}_{UN}$ moles/l	ti sec	Δt sec	D x 10^6 cm^2/sec	$(\bar{D} \pm \Delta D) \times 10^6$ cm^2/sec
7A1	0.02	0.896	769	77	1.415	
7A2	0.02	0.896	789	120	1.336	1.376±.027
7A4	0.02	0.896	727	119	1.378	
7B1	0.02	0.753	615	83	1.620	
7B2	0.02	0.753	624	96	1.592	1.590±.022
7B3	0.02	0.753	616	88	1.556	
7C1	0.02	0.519	900	151	1.511	
7C2	0.02	0.519	868	153	1.524	1.515±.023
7C3	0.02	0.519	811	133	1.510	
7D1	0.02	0.300	655	144	1.756	
7D2	0.02	0.300	665	153	1.524	1.515±.006
7D3	0.02	0.300	667	142	1.711	
7E1	0.019	0.200	291	85	2.121	
7E2	0.019	0.200	292	83	2.087	2.054±.07
7E3	0.019	0.200	329	67	1.955	
7F2	0.02	0.100	407	118	1.937	1.913±.024
7F3	0.02	0.100	409	122	1.889	
7G1	0.02	0.05	451	130	2.012	
7G2	0.02	0.05	392	122	2.042	1.992+.046
7G3	0.02	0.05	390	149	1.923	
7P1	0.02	0.01	452	123	2.119	
7P2	0.02	0.01	456	147	1.986	2.018±.067
7P3	0.02	0.01	455	150	1.949	

TABLE V

DIFFUSION COEFFICIENT AT 25°C FOR THE SYSTEM URANYL NITRATE IN 100 V/V % TRIBUTYL PHOSPHATE

Run. No.	ΔC_{UN} moles/l	$\bar{C}_{UN}$ moles/l	ti sec	Δt sec	$D \times 10^6$ cm^2/sec	$(\bar{D} \pm \Delta D) \times 10^6$ cm^2/sec
10A2	0.02	0.01	1489	509	0.760	0.826 ± 0.066
10A3	0.02	0.01	1469	340	0.892	

TABLE VI

DIFFUSION COEFFICIENTS AT 25°C FOR THE SYSTEM URANYL NITRATE TRIBUTYL PHOSPHATE COMPLEX IN 100 V/V % N HEPTANE

Run No.	ΔC_{UN} moles/l	$\bar{C}_{UN}$ moles/l	ti sec	Δt sec	$D \times 10^6$ cm^2/sec	$(\bar{D} \pm \Delta D) \times 10^6$ cm^2/sec
0A1	0.02	0.01	358	66	8.143	8.171±.028
0A2	0.02	0.01	362	70	8.199	

solution was used. The uranyl nitrate concentration, $\bar{C}_{UN}$, corresponds to the average value of the upper and lower solution concentrations. The second column is the difference between the upper and lower solution concentrations at the start of the diffusion run. The last column are the mean values of D taken from the individual D values for runs with the same first number and letter, and the corresponding average absolute deviation, ΔD.

A uniform concentration gradient of 0.02 moles/liter uranyl nitrate had been used for most of the runs. Since the variation of the diffusion coefficients with uranyl nitrate concentration is small, as shown by the data, with $\Delta C = .02$ moles/l, the assumption of a constant diffusion coefficient, D, in the derivation of Equation (V-1) (8) is justified for this study. The diffusion coefficients are effectively differential diffusion coefficients because of the small gradient employed. The linear relationship between the refractive index and uranyl nitrate concentration in TBP diluent systems have been verified by Slansky (72).

As noted in Chapter II, the experimental diffusion coefficients presented here are defined by the equation:

$$N_1 = -D\frac{\partial C_1}{\partial x} \qquad \text{(II-5a)}$$

This equation may also be written in the form:

$$N_1 = -D^1 \frac{\partial C_1}{\partial x} + Cv^o \qquad \text{(V-6)}$$

where D' = coefficient of "true" diffusion as represented by the first term of the equation

v° = volume average velocity of the bulk

Cv° = contribution to the flux due to bulk flow

In the diffusion cell used in this study, bulk flow will be introduced if there is an appreciable volume change in the solution during diffusion. This would physically be manifested by a vertical displacement of the interface. Based on V = 606 cm^3/mole for $UO_2(NO_3)_2 \cdot 2 \cdot TBP$ (62), it is estimated that the volume change is about 0.1 cm^3 or 0.4% of the total cell volume. A displacement of the interface has not been detected in any of the runs. It may be assumed that the contribution of the bulk flow to the flux is negligible. In this case the two diffusion coeffecients defined by Equations (II-5a) and (V-6) become equivalent. The diffusion coefficient defined by Equation (V-6) is also equivalent to that defined by:

$$J_1 = C(\bar{v}_1 - \bar{v}^\circ) = -D' \frac{\partial C_1}{\partial x} \qquad (V-7)$$

The theoretical discussions of the diffusion process found in literature are based on Equation (V-7).

Density and Viscosity Data

Table VII, presents experimental density and viscosity data at 25°C. for all the systems studied. The experimental density data for each of the tributyl phosphate-n heptane combination were fitted by a linear regression program to

TABLE VII

DENSITY AND VISCOSITY DATA AT 25°C

C_{UN} moles/l	ρ gm/ml	C_{UN} moles/l	μ cp
URANYL NITRATE IN 30 V/V % TBP - 70 V/V % N HEPTANE			
0.0	0.7772	0.0	0.659
0.015	0.7819	0.01	0.655
0.079	0.8037	0.05	0.674
0.172	0.8356	0.10	0.714
0.313	0.8723	0.200	0.775
0.359	0.8853	0.300	0.837
0.450	0.9282	0.401	0.935
0.480	0.9353	0.481	0.954
0.482	0.9363		
URANYL NITRATE IN 50 V/V % TBP - 50 V/V % N HEPTANE			
0.0	0.8197	0.0	0.981
0.05	0.8335	0.01	0.996
0.20	0.8874	0.05	1.042
0.35	0.9400	0.100	1.102
0.50	0.9865	0.200	1.214
0.754	1.0609	0.350	1.535
0.910	1.1065	0.500	1.781
		0.750	2.367
		0.900	2.867

TABLE VII (Cont.)

C_{UN} moles/l	ρ gm/ml	C_{UN} moles/l	μ cp
URANYL NITRATE IN 70 V/V % TBP - 30 V/V % N HEPTANE			
0.0	0.8867	0.0	1.681
0.1127	0.9177	0.01	1.707
0.1870	0.9450	0.05	1.778
0.384	1.0034	0.100	1.885
0.767	1.1121	0.200	2.100
0.978	1.1656	0.300	2.374
		0.519	3.139
		0.753	4.347
		0.896	4.934

the following equations as functions of the uranyl nitrate concentration:

$$= 0.776 + 0.328\ C_{UN} \quad \text{for 30 V/V percent TBP-70\% n-heptane}$$

$$= 0.882 + 0.317\ C_{UN} \quad \text{for 50 V/V percent TBP-50\% n-heptane}$$

$$= 0.889 + 0.287\ C_{UN} \quad \text{for 70 V/V percent TBP-30\% n-heptane}$$

(V-8)

CHAPTER VI

DISCUSSION OF RESULTS

The discussion of results is divided into four parts. At the beginning, an analysis of the sources of error in the determination of the diffusion coefficients is presented. Then a discussion of the variation of the diffusion coefficients with uranyl nitrate concentration and with tributyl phosphate dilution follows. The third part is a comparison of the experimental data obtained in this study with available correlations. A generalized plot of all the experimental data is presented at the end of the chapter.

Error Analysis

In the method employed in this study, the following factors contribute to the uncertainty of the calculated diffusion coefficients:

(a) experimental error in the measurement of the distance between the interference fringes

(b) errors arising from non-ideal and non-uniform boundary formation

(c) variation in temperature

(d) experimental error in the determination of the magnification factor.

(e) experimental error in recording of time.

Each reported data point is the average of two or three consecutive runs. The reproducibility is affected by factors (a) through (e) and the accuracy of the reported value is a direct function of (d).

Since the diffusion coefficient, D, was calculated as a parameter from a curve fit of several (2x) and t measurements, the contribution to the uncertainty due to (a) was set equal to the estimate of the standard error of D, $\hat{s}_D$, in the curve fit. The estimate of the standard error of the parameter was calculated according to the method by Box (7). The details of the calculation is given in Appendix B.

Another source of error between diffusion runs is non-uniform boundary formation. An approximate information was obtained from the differences in calculated values of Δt and t_i between runs of identical solutions. The temperature was controlled to $\pm$ .005°C. It was assumed that the contribution to the error due to temperature variation is negligible. Since the average duration of an experimental run is over ten minutes, the experimental error due to time measurement, approximately one second, is negligible. The final expression for the per cent standard deviation in the calculated diffusion coefficients was obtained as:

$$\frac{s_D}{D} = \sqrt{\left(\frac{\hat{s}_D}{D}\right)^2 + \left(\frac{s_{\Delta t}}{t_i+\Delta t}\right)^2 + \left(\frac{s_{ti}}{t_i+\Delta t}\right)^2 + \left(\frac{s_{MF}}{MF}\right)^2} \qquad \text{(VI-1)}$$

The derivation of Equation (VI-1) is given in Appendix B.

Using calculated values of s_D, s_{Dt} and s_{ti} for Run Numbers 3I, 5A and 7C (Appendix B), Equation (VI-1) gives 5.0%, 3.0% and 3.0% respectively. The limiting factor in the calculation are those involving $s_{\Delta t}$ or s_{ti}. The analysis of error show higher per cent standard deviation than the experimental data which are 4%, 2% and 0.4%. The order of magnitude of the experimental standard deviation is closer to the estimate of the standard error of the parameter D, obtained from the curve fit (first term in Equation (VI-1). It is most probable that the assumption used in the calculation of the contribution of Δt and t_i to the experimental error (Appendix B) tend to overestimate their actual contribution.

The average standard deviation for all the runs are $\pm$ 1.3% ($\pm$ .05 x 10^{-6} cm^2/sec) for the 30 V/V % TBP series, $\pm$ 1.7% ($\pm$ .04 x 10^{-6} cm^2/sec) for the 50 V/V % TBP series, and $\pm$ 2.0% ($\pm$ .04 x 10^{-6} cm^2/sec) for the 70 V/V % TBP series.

The increase in the per cent standard deviation from the 30 V/V % TBP series to the 70 V/V % TBP series is due to decreasing values of the diffusion coefficients D.

The accuracy of the data is determined by the

experimental error of the magnification factor used and the experimental error in the analytical determination for the uranyl nitrate. The experimental error in the determination of the concentration c_{UN}, obtained by the ferrocyanide technique (22) was $\pm$ 0.3%.

The magnification factor was calculated from a standard diffusion run using an aqueous solution of NaCl. From an analysis of error similar to that described above, the per cent standard deviation is $\pm$ 0.4%. The limiting factor in the calculation was the estimate of the standard error of the parameter MF in the curve fit (Appendix B). The excellent agreement of the data for the magnification factor runs, $\pm$ 0.12%, may be fortuitous. From an independent estimate of the magnification factor using measurements of the dimensions of the cell cavity, (Appendix B), the agreement with the magnification factor runs was $\pm$ 1.4%.

The experimental error of the density and viscosity measurements were both $\pm$ 0.5%.

Variation of the Diffusion Coefficients with Uranyl Nitrate Concentration and with Tributyl Phosphate Dilution

First, it is important to establish the chemical species present in the system under study. For the purpose of this experiment it was found sufficient to make a single analytical determination for the solution, that of the uranium concentration. Literature studies (35, 39, 42)

have shown that the solution of uranyl nitrate in tributyl phosphate-diluent consists of the following species: The disolvate $UO_2(NO_3)_2 \cdot 2TBP$ in an anhydrous, practically undissociated state, the "free" or unbounded tributyl phosphate, the diluent, and water whose nature in the system is not clear. The existence of the compound $TBP \cdot H_2O$ has been postulated (3, 39, 60) but in the presence of uranyl nitrate and inert diluents the amount of water present is not the correct stoichiometric value to correspond to the free tributyl phosphate concentration (14). In the discussion that follows water is not considered as a separate component. It is instead incorporated with the free TBP, by saying that this component is present as water-saturated TBP.

The Variation of the Diffusion Coefficients with Uranyl Nitrate Concentration

$\bar{D}$ and $\bar{C}_{UN}$ from Tables II, III and IV are plotted in Figure 6. A smooth decreasing line may be drawn through the experimental points for the system 70 V/V% TBP and also for the 50 V/V% TBP. The diffusion coefficients for Run 7E lie above the smooth curve drawn for the 70 V/V% TBP system. This may be explained by the comparatively short duration of the diffusion time for this run. A gradient of $C_{UN} = .019$ moles per liter was used. In diffusion runs of smaller concentration gradient, the disturbances due to the boundary formation process i.e., turbulence or

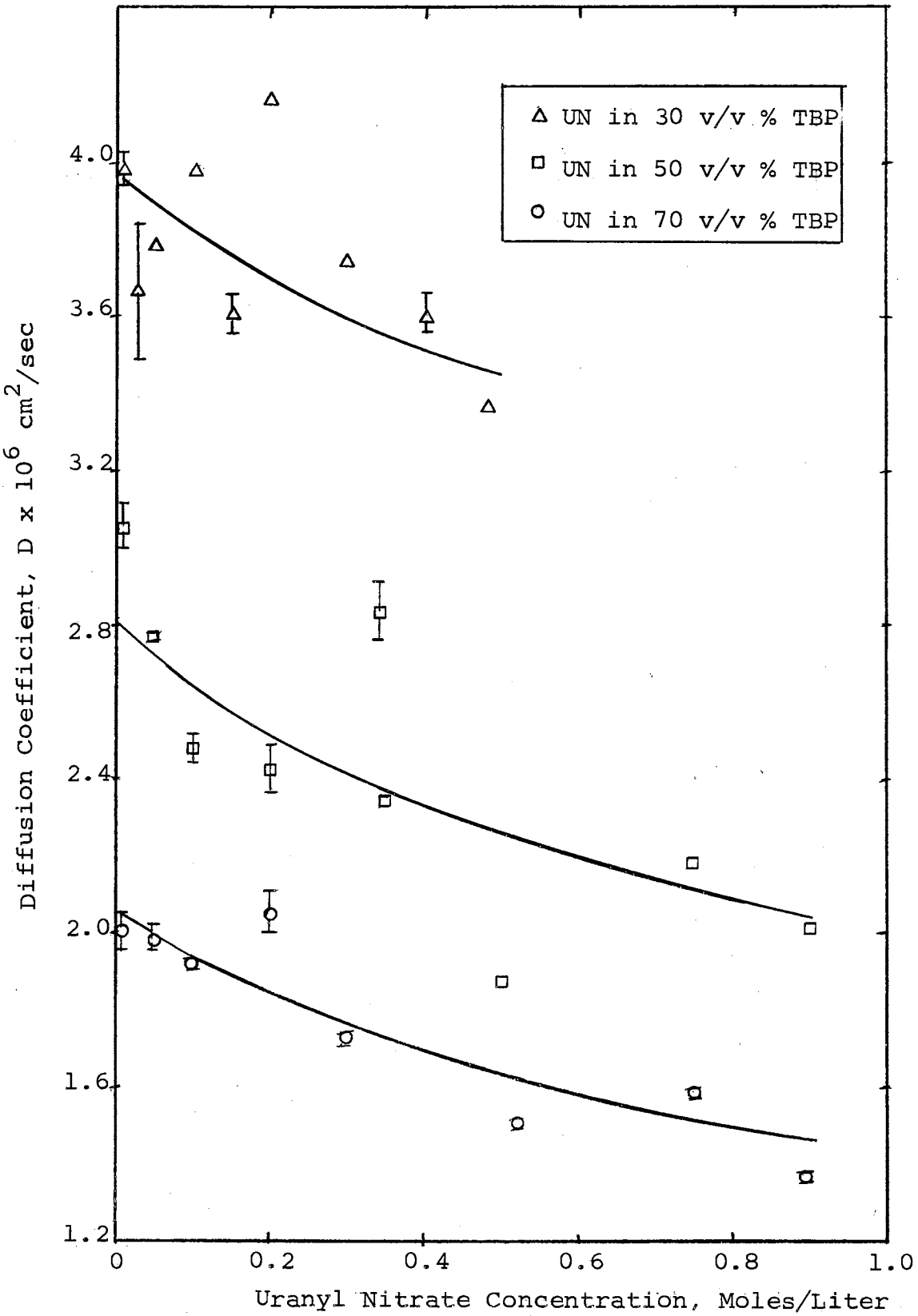

Figure 6. Variation of Diffusion Coefficient with Uranyl Nitrate Concentration

skewness, die out more slowly. It is very likely that measurements of the fringe pattern were taken before these effects have completely disappeared. Although there was no visible evidence of instability in the initial interface formed it is also possible that the system was more sensitive to very small temperature gradients or vibrations which cannot be totally be eliminated in the apparatus.

The same reasoning applies to the experimental run 5H (C_{UN} = .018). In this case, however, the diffusion coefficient lie below the smooth curve for the 50 v/v% TBP series. The observation from runs 7E and 5H then imply that it is not possible a priori, to say if the boundary formation effects cause an increase or a decrease in the measured diffusion coefficients. The unusually large departure of run 5A from the smooth curve may be attributed to some bias introduced in the measurement of the fringe distance between the fringes. The photographs for Run 5A have darker background (i.e., less contrast with the fringe pattern) than most other photographs of diffusion runs made. This was due to the use of a freshly prepared film developing solution (the film developer had been allowed to stand as required, for 24 hours, but run 5A was the first film developed with the solution). The uncertainty and probable error in locating the proper dark fringe maxima is also attested by the large experimental error obtained for Run 5A ($\pm$ 0.113). A check, run 5I was made from the same stock solution from which 5A was prepared and performed three

days later. It failed to duplicate the high value of the diffusion coefficient for run 5A.

The trend exhibited by the diffusion coefficient for the 30 V/V % TBP series is not very clear due to the considerable scatter of the data obtained. Runs 3A to 3G were performed at the beginning of the experimental project. At that time the data seemed to indicate the presence of both a minima and a maxima, runs 3F and 3D respectively. Four months later runs 3I and 3P, prepared from the same stock as that used for runs 3D and 3E, were made. The diffusion coefficients obtained did not duplicate these extrema. The large experimental error of run 3P may be due to the slight weakening of the intensity of the laser beam which made readings of the fringe pattern more difficult.

Some doubts based on these checks may, however, be raised. Experimental studies (12) have shown that TBP undergoes degradation in the presence of water and uranyl nitrate. The effect of the latter is minimized if the solution is stored away from light, as was done in this study. It is assumed that the only measurable degradation product is dibutyl phosphate. Based on published data on the rate constant of the hydrolysis reaction (12), in the four month period, in 30 v/v% TBP, .006 moles of dibutyl phosphate will form, about .6% of the total TBP concentration. Dibutyl phosphate exists in solution as the complex $UO_2(NO_3)_2 \cdot 2DBP$ or as free dibutyl phosphate or both. One

cannot say at this point if this calculated amount of dibutyl phosphate formed will cause a perceptible change in the diffusion coefficient of the mixture.

The photograph obtained for Run 3E had a similar poor contrast quality as that of run 5A. Although the experimental error of Run 3E is within the range of the average experimental error, the large value of D may have been caused by a reproducible bias in the measurement of the fringe pattern. No irregularity in the experiment has been detected for Run 3D. The use of this single point as a valid trend for the 30 V/V% TBP series is, however, questioned. This conclusion is influenced by the data for the system at 50 V/V% and 70 V/V% TBP, where a smooth decreasing diffusion coefficient with increasing uranyl nitrate concentration is clearly evident. The available literature on the subject (35, 39, 42) show that the specie $UO_2(NO_3)_2 \cdot 2TBP$ is not altered by the dilution of TBP with hydrocarbon diluents.

The existence of extrema in a diffusion coefficient-composition plot has been attributed (80) to strong interaction between the species in solution, causing highly non-ideal thermodynamic behavior or formation of associated molecules. To date no complete thermodynamic study has yet been made on the ternary system uranyl nitrate-TBP-diluent. Aartsen and Korveze (1) concluded from an extraction study on uranyl nitrate-TBP-carbon tetrachloride, that at TBP dilutions from 0-50 V/V% by volume, the system

may be considered ideal at uranyl nitrate concentrations below 0.6 moles/liter. However, their proof is not conclusive. In their equation, the ratio of the activity coefficients of uranyl nitrate and TBP becomes unity, not the individual activity coefficients.

The thermodynamic characterization of a binary solution is usually qualitatively shown by logarithmic plots of viscosity against mole fraction. A linear relationship is often used as criteria for ideal classification (36). This is based on Eyring's model of viscous flow and the linear additivity of the pure component free energies of activation (28). It would seem that if there are no strong interactions between the components present in solution, the properties of the mixture may be approximated by a suitable relationship of their pure component properties, Figure 7 shows that the viscosity of the 30 V/V % TBP mixture is almost linear with molar concentration. Since the diluent concentration is constant for each TBP dilution series, Figure 8 shows a plot of the solution viscosities and a normalized composition abcissa based on the components with changing composition. The system at 30 V/V % TBP exhibits the least deviation from a linear rule.

Burchard and Toor (11) have studied diffusion in some thermodynamically ideal ternary systems. They have found that the multicomponent diffusion coefficient may be expressed as a linear function of the component mole fractions. Unfortunately, the 30V/V % TBP data show consider-

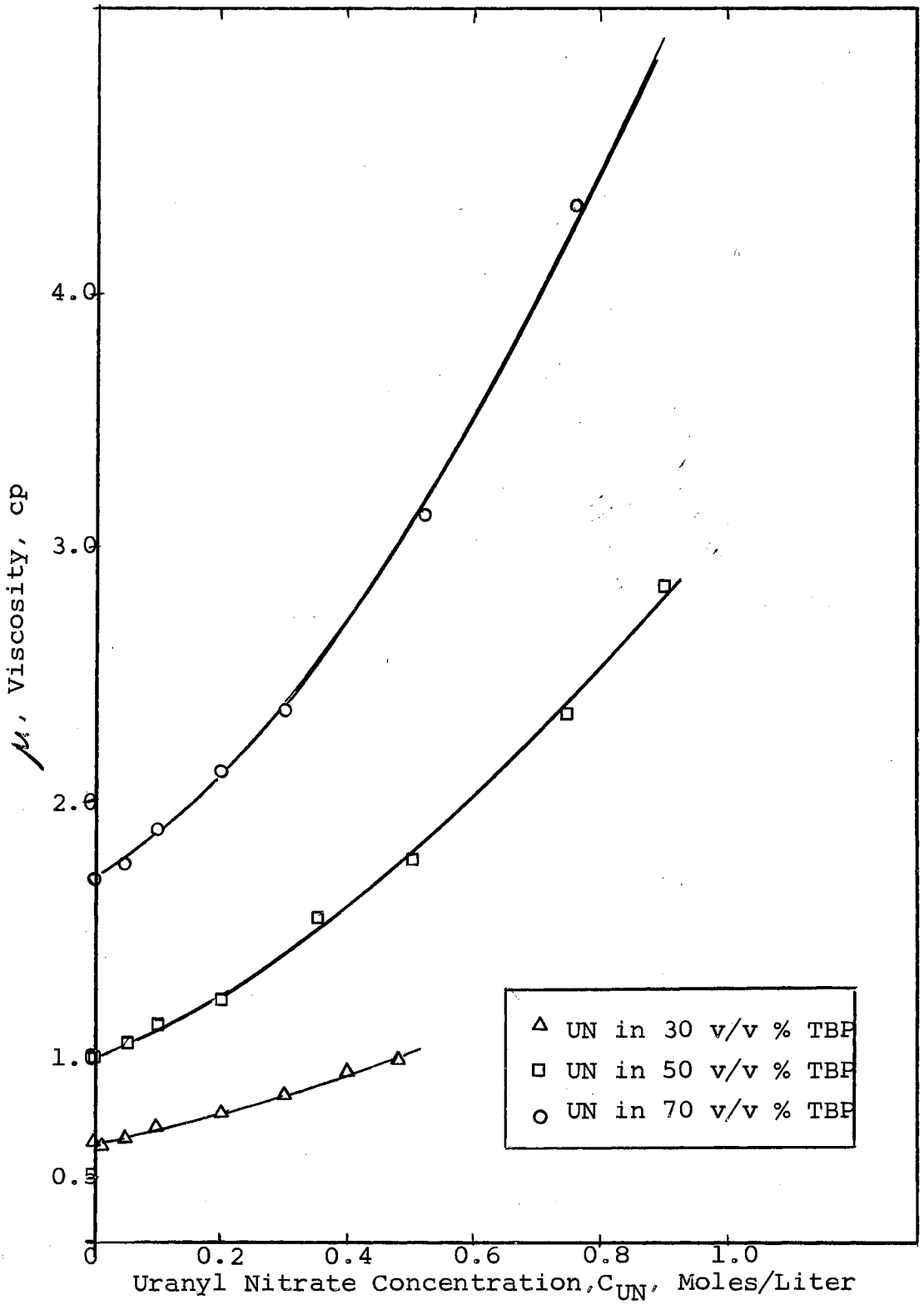

Figure 7. Variation of Solution Viscosity with Uranyl Nitrate Concentration

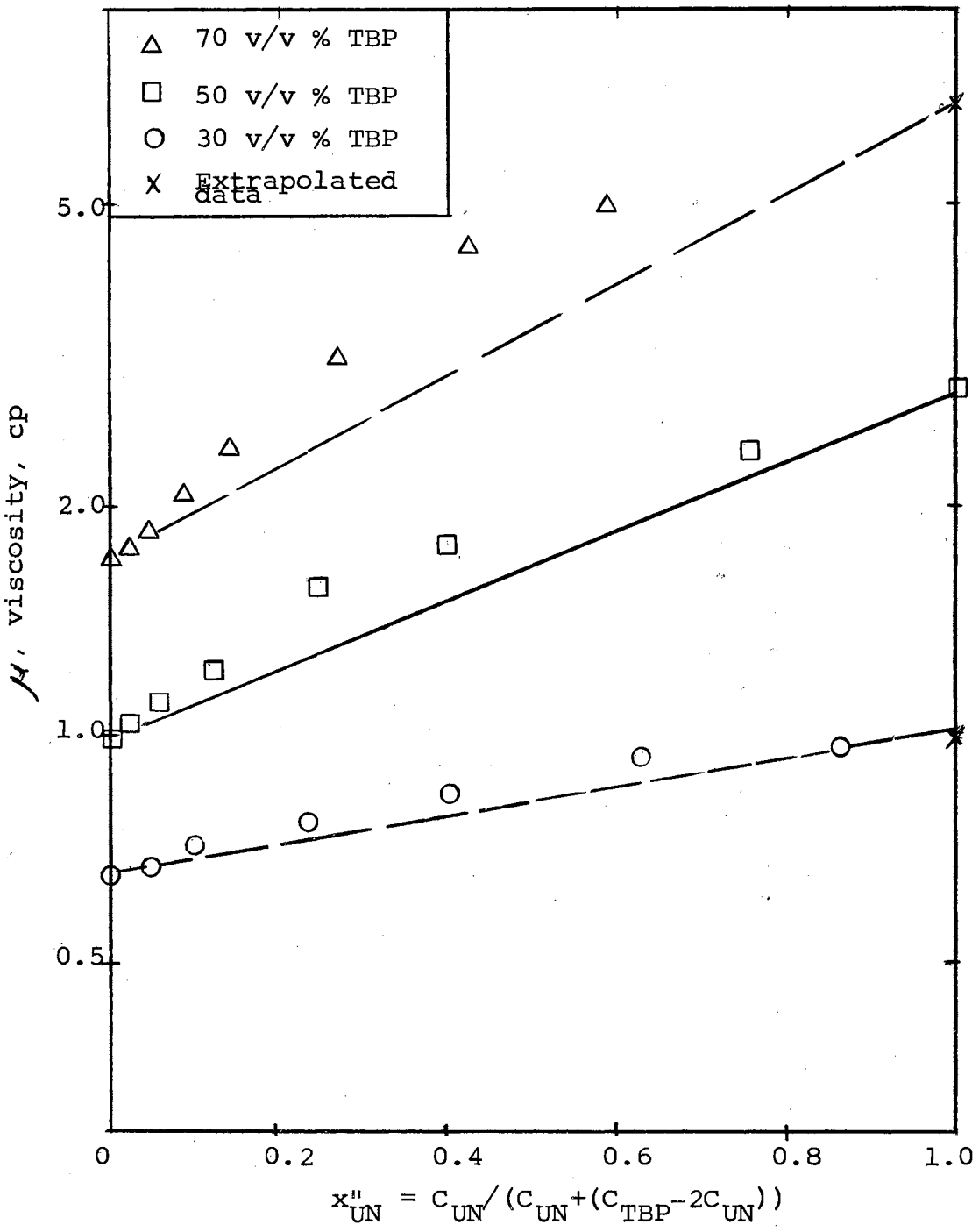

Figure 8. Variation of Solution Viscosity with Mole Fraction Uranyl Nitrate (Heptane Free Basis)

able scatter and preclude any comparison.

Based on the above discussion the author believes that the shape of the diffusion coefficient-composition plot for all the systems studied here i.e., 30, 50 and 70 V/V % TBP, are similar, as shown in Figure 6. The data indicate a rapid decrease in D at small uranyl nitrate concentrations but a partial levelling off of the curve at C_{UN} approaching saturation concentration. This may be explained in terms of the species present and their interactions. Statistical-mechanical theories show that molecular interactions determine the friction coefficient, ζ_{ij}, which is inversely related to the diffusion coefficients (4). If one assumes that the diffusion coefficient is a function only of unlike pairwise interactions, the following interactions affect the system: $UO_2(NO_3)_2 \cdot 2TBP$-TBP, $UO_2(NO_3)_2 \cdot 2TBP$-n-heptane, TBP-n-heptane. At increasing uranyl nitrate concentration, C_{UN}, the diffusion coefficients decrease due to the rise of the $UO_2(NO_3)_2 \cdot 2TBP$-solvent interactions. However, the increase of uranyl nitrate concentration is also accompanied by a decrease in the "free" TBP concentration. At C_{UN} near saturation, only the species $UO_2(NO_3)_2 \cdot 2TBP$ and normal heptane are in appreciable amount. At this point, the contributions to the resistance to diffusion due to $UO_2(NO_3)_2 \cdot 2TBP$-TBP, and TBP-n-heptane interactions vanish. The above discussion may be an oversimplified picture. The assumption is that the friction coefficient may be given in terms

of additive pairwise interactions. These types of interactions are further discussed in the following section.

The Effect of Tributyl Phosphate Dilution on Diffusion Coefficients

Figure 6, also shows that the diffusion coefficients increase with increase in TBP dilution. Studies on solvent effects in diffusion (28), correlate the diffusion coefficients with the viscosities of the solvents or the solutions. The variation of the viscosity product $D\mu$ is shown in Figure 9. There is a good comparison between the shapes of these curves and that of the curves of μ against C_{UN} as shown in Figure 7.

The modified theory of Olander (51) has been successful in the prediction of the viscosity product for dilute binary systems. According to the formulation:

$$Y = \left(\frac{D\mu}{T}\right)\left(\frac{\varepsilon}{k}\right)\left(\frac{V}{N_{av}}\right)^{1/3} = \exp\left(\frac{\Delta G_{\mu}-\Delta G_{D}}{RT}\right) \qquad \text{(II-20)}$$

$$\text{or} \quad Y = f\delta = \exp\left(\frac{\Delta G_{\mu}-\Delta G_{D}}{RT}\right)$$

Figure 10, shows a plot of ln Y v. δ for the system under study at $\bar{c}_{UN} = .01$. The activation energy term, δ, was calculated using the mole fraction average of δ_T and δ_H, of the solvents TBP and n-heptane respectively. V was also calculated as the mole fraction average of V_T and V_H. The necessary calculations are shown in Appendix C. The data may be represented by a straight

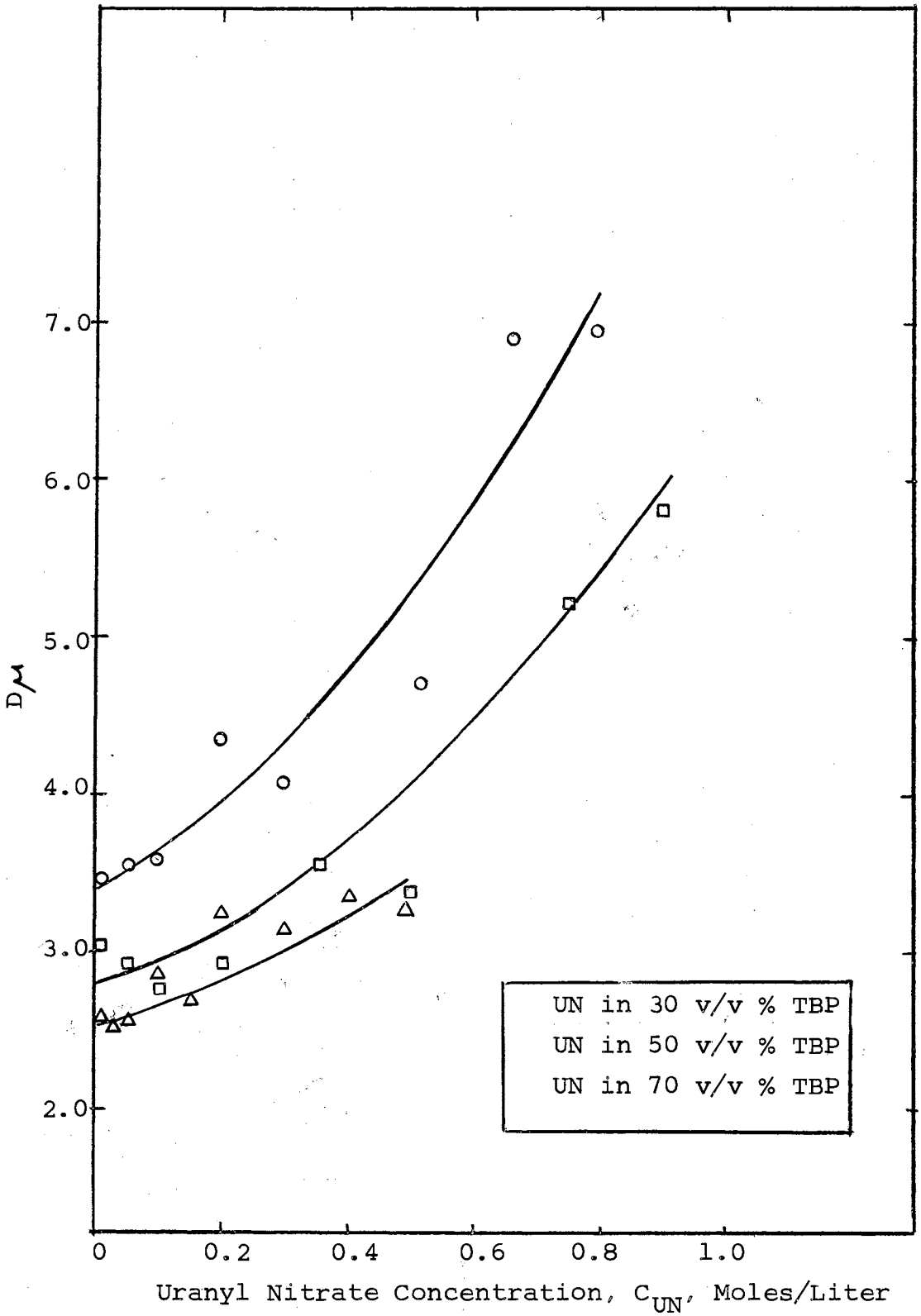

Figure 9. Variation of Diffusivity-Viscosity Product with Uranyl Nitrate Concentration

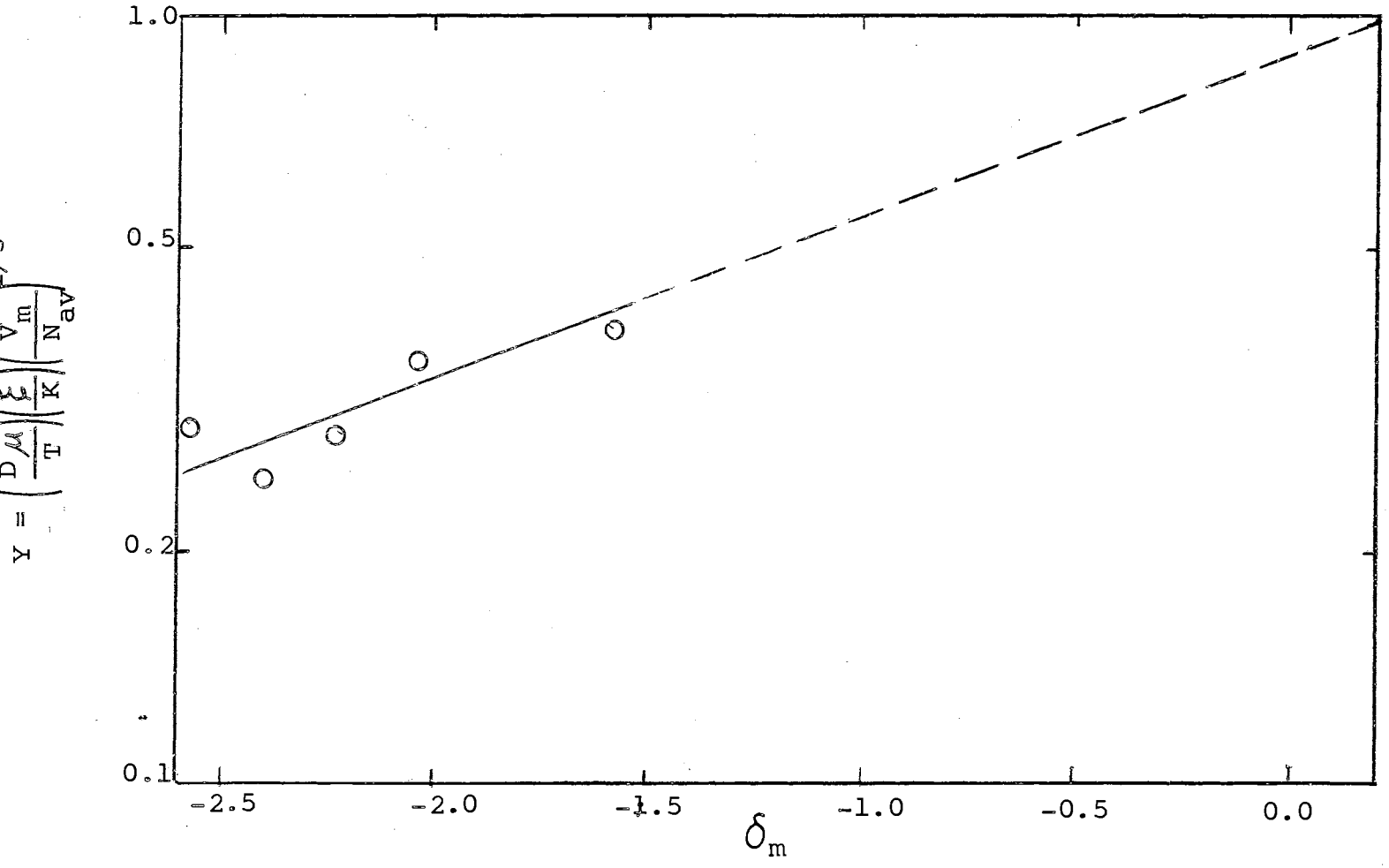

Figure 10. Effect of Tributyl Phosphate Dilution on the Diffusivity-Viscosity Product

line of slope equal to 0.48. The fraction of the total activation energy for the viscous process which is due to the kinetic or jump step for this system is therefore close to the average value of 1/2 found for several binary systems by Olander (51). The negative values of δ are due to the fact that the solute is more viscous and has a greater molar volume than either of the solvents or their combination. The deviation of the line from the theoretical value of Y = 1.0 at $\delta = 0$ may be attributed to the choice of $\xi = 6.0$.

If an oversimplified view is taken of the activation energy term $f\delta$, the first term represents activation energy required to break solvent-solvent interaction and the second term represents activation energy necessary to overcome solute-solvent interaction. For a solvent which is a mixture of two components, if there is no significant interaction between components, a weighted average of the pure component activation energies can be used to represent the overall interaction. The equations for δ may therefore be written as:

(VI-2)

$$\delta = X_T \Delta G_{TT} + X_H \Delta G_{HH} - \left(X_T \sqrt{\Delta G_{TT} \Delta G_{U2T}} - X_H \sqrt{\Delta G_{HH} \Delta G_{U2T}} \right)$$

$$= X_T \left(\Delta G_{TT} - \sqrt{\Delta G_{TT} G_{U2T}} \right) + X_H \left(\Delta G_{HH} - \sqrt{\Delta G_{HH} \Delta G_{U2T}} \right)$$

(VI-3)

The latter equation was used to evaluate δ. In the discussion a direct relation had been implied for the interaction energies and the activation energies defined by the rate theory. A more rigorous treatment similar to the approach used by Gainier and Metzner (27) will probably give a better insight, but will require thermodynamic data that are not yet available for the solute $UO_2(NO_3)_2 \cdot 2TBP$.

Figure 10, therefore, seems to indicate that no significant interaction is present in the mixed solvents. The solution may be treated as a pseudobinary, with the properties of the solvent taken as the mole fraction average of its components. The effect of the dilution of TBP on the viscosity product is to alter the solvent properties to correspond to the mole fraction average of the TBP and the diluent.

For the behavior of the diffusion coefficients alone, using the assumed mixing rule in the Eyring equation, one obtains:

$$D_{1m} = \frac{\left(V_m/N_{av}\right)^{2/3}}{\delta} \frac{kT}{\left(2\pi m_1 kT\right)^{1/2}} \frac{1}{\left(V_{f1m}\right)^{1/3}} e^{-\left|\Delta G_{1m}/RT\right|} \qquad \text{(VI-4)}$$

$$= \frac{\left(V_m/N_{av}\right)^{2/3}}{\delta} \frac{kT}{\left(2\pi m_1 kT\right)^{1/2}} \frac{1}{\left(V_{f1m}\right)^{1/3}} e^{-\left|\frac{x_T \Delta G_{1T} + x_H \Delta G_{1H}}{RT}\right|}$$

Here ΔG, represents the total activation energy for diffusion. Since

$$\mathcal{D}_{1T} = \frac{(V_T/N_{AV})^{2/3}}{\zeta} \frac{KT}{(2\pi m_1 KT)^{1/2}} \frac{1}{(V_{f1T})^{1/3}} e^{-\Delta G_{1T}/RT} \qquad \text{(VI-5)}$$

if the assumption is made that the pre-exponential term does not change much with TBP dilution, the equation reduces to:

$$D_{1m} = (\mathcal{D}_{1T})^{X_T} \quad (\mathcal{D}_{1H})^{X_H} \qquad \text{(VL-6)}$$

This is the same equation for binary systems arrived at by Cullinan (18) using a combination of the phenomenological equations of transport and the rate theory, and by Vignes (80) from empirical analysis.

Figure 11 shows a plot of ln D against mole fraction heptane. The theory predicts a straight line joining the diffusion coefficients of the pure solvent system. The data at intermediate TBP dilutions indicate a slight curvature. If the pure solvent binary diffusion coefficients obtained are slightly higher than their actual value, this curvature is diminished. The possibility of a displacement has not been detected but it cannot also be ruled out. It must also be pointed out that the system $(UO_2(NO_3)_2 \cdot 2TBP$ in 100% n- heptane is almost water-free compared to all the other water-containing systems.

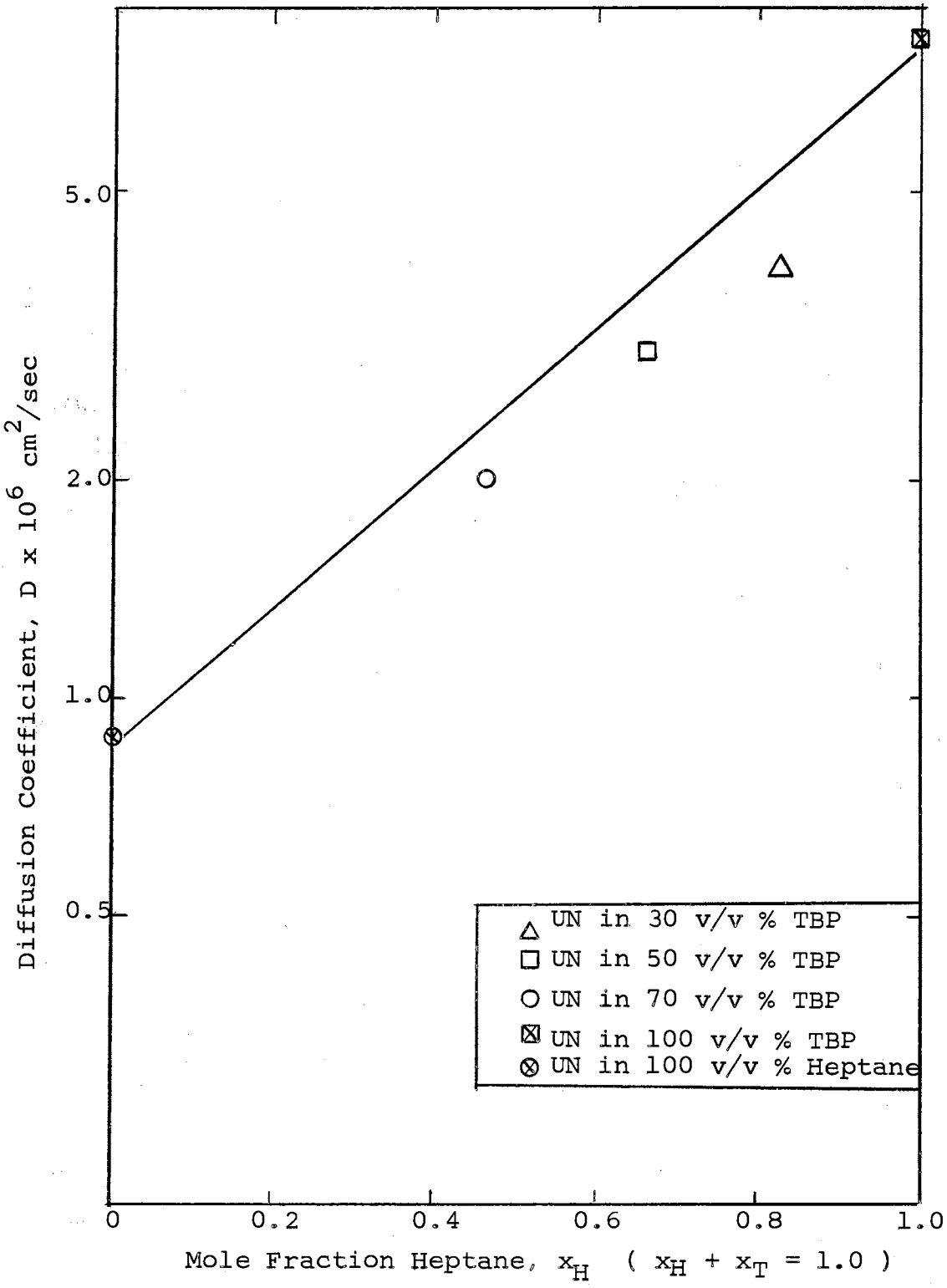

Figure 11. Variation of Diffusion Coefficient with Tributyl Phosphate Dilution

In all of the above calculations, the properties attributed to TBP were those for water saturated TBP. It was assumed that water was bonded to TBP. An extreme view of the presence of free water in the solution may also be taken and the solvent be treated as a three component system. However, no analytical determination for the water content has been made in this study. Furthermore, there are no appropriate data available for the binary mixture of $UO_2(NO_3)_2 \cdot 2TBP\text{-}H_2O$. In view of the complex nature of the system used in this study and the assumption made regarding its composition, the amenability of the data to treatment based on simple binary models is surprising.

Interaction Effects in the System Uranyl Nitrate-Tributyl Phosphate-n-Heptane System

Literature studies (54, 56, 67) indicate that the organic solutions of uranyl nitrate form non-ideal solutions. There are, however, no thermodynamic data for the three component system to fully characterize the behavior of the solution. An insight may be provided by looking at the extent of pairwise interactions of the components present. A rough test of the interaction strength may be obtained by plotting the diffusion coefficient or the logarithm of the mixture viscosity against mole fraction. Literature data (28, 36) has shown that for ideal binary mixtures, plots of this type are generally linear, while

pronounced non-ideality or association effects usually result in extensive curvature.

Figure 12, is a plot of the logarithm of the viscosity against mole fraction for the solvent mixture TBP-n-heptane. The data show nearly linear behavior and may be taken to indicate that the TBP-n-heptane interaction are due to weak dispersion forces only.

A similar plot for the binary mixture of $UO_2(NO_3)_2 \cdot 2TBP$-n-heptane is given in Figure 13. The points at the intermediate mole fractions represent the system uranyl nitrate-n V/V % TBP-n heptane when saturated with respect to uranyl nitrate concentration. The viscosity of pure $UO_2(NO_3)_2 \cdot 2TBP$ was taken from the data by Healy and McKay (35). The data show more curvature than that exhibited in the TBP-n heptane mixture. However, it must be noted that in theory, a saturated solution of uranyl nitrate-TBP-n heptane contains no free TBP. In practice complete saturation is seldom attained and some free TBP may still exist in solution.

The viscosity data for the water saturated solution of uranyl nitrate in TBP by Healy and McKay (35) is similarly plotted, Figure 14. The data also show mild curvature, the deviation from linear behavior of similar extent as that in the $UO_2(NO_3)_2 \cdot 2TBP$-n heptane. It is probable that a weak dipole force exists between the $UO_2(NO_3)_2 \cdot 2TBP$ molecules and those of TBP and n-heptane.

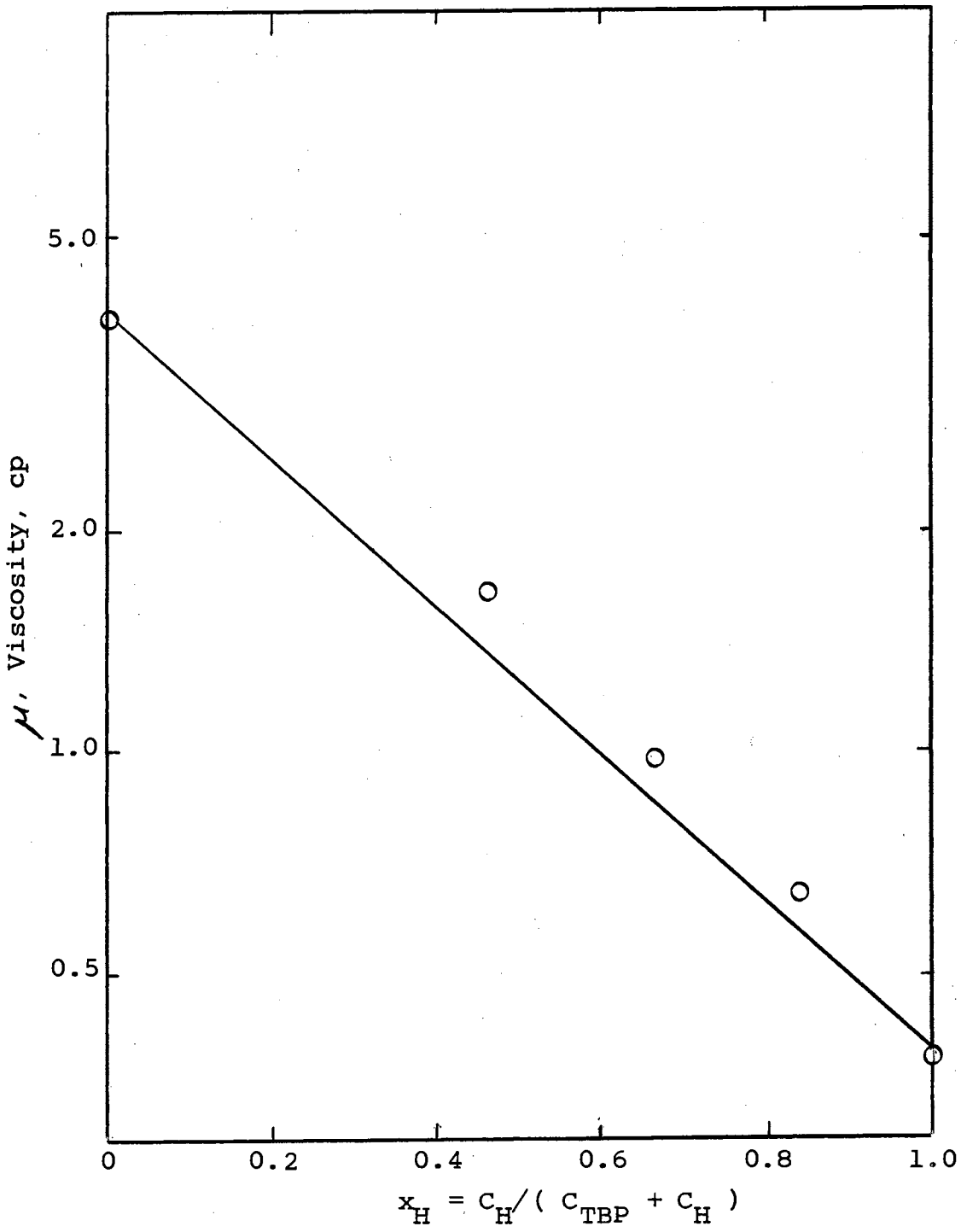

Figure 12. Variation of Solution Viscosity with Mole Fraction n-Heptane in the TBP-n-Heptane Binary

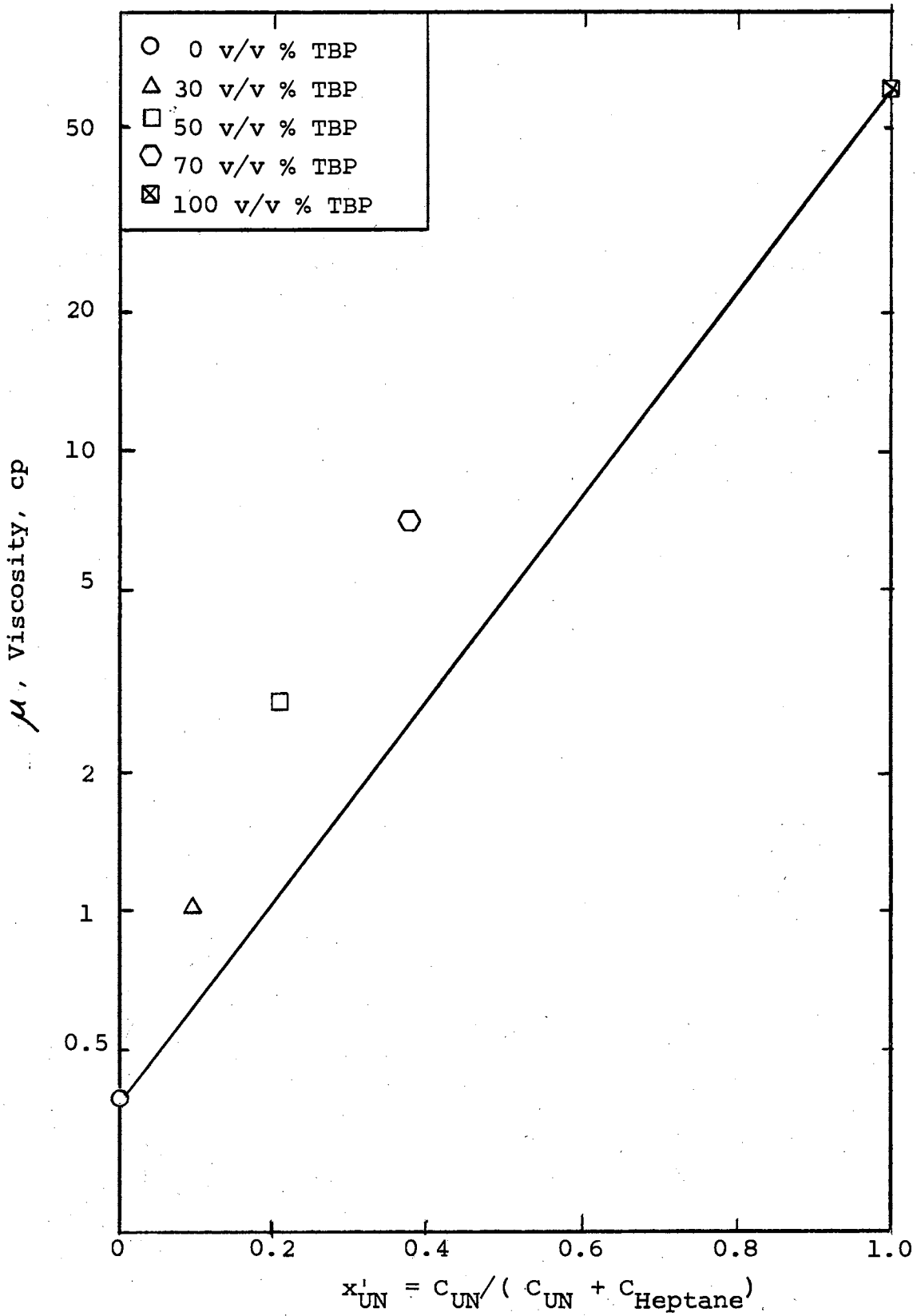

Figure 13. Variation of Solution Viscosity with Mole Fraction UN in the UN.2TBP-n-Heptane Binary

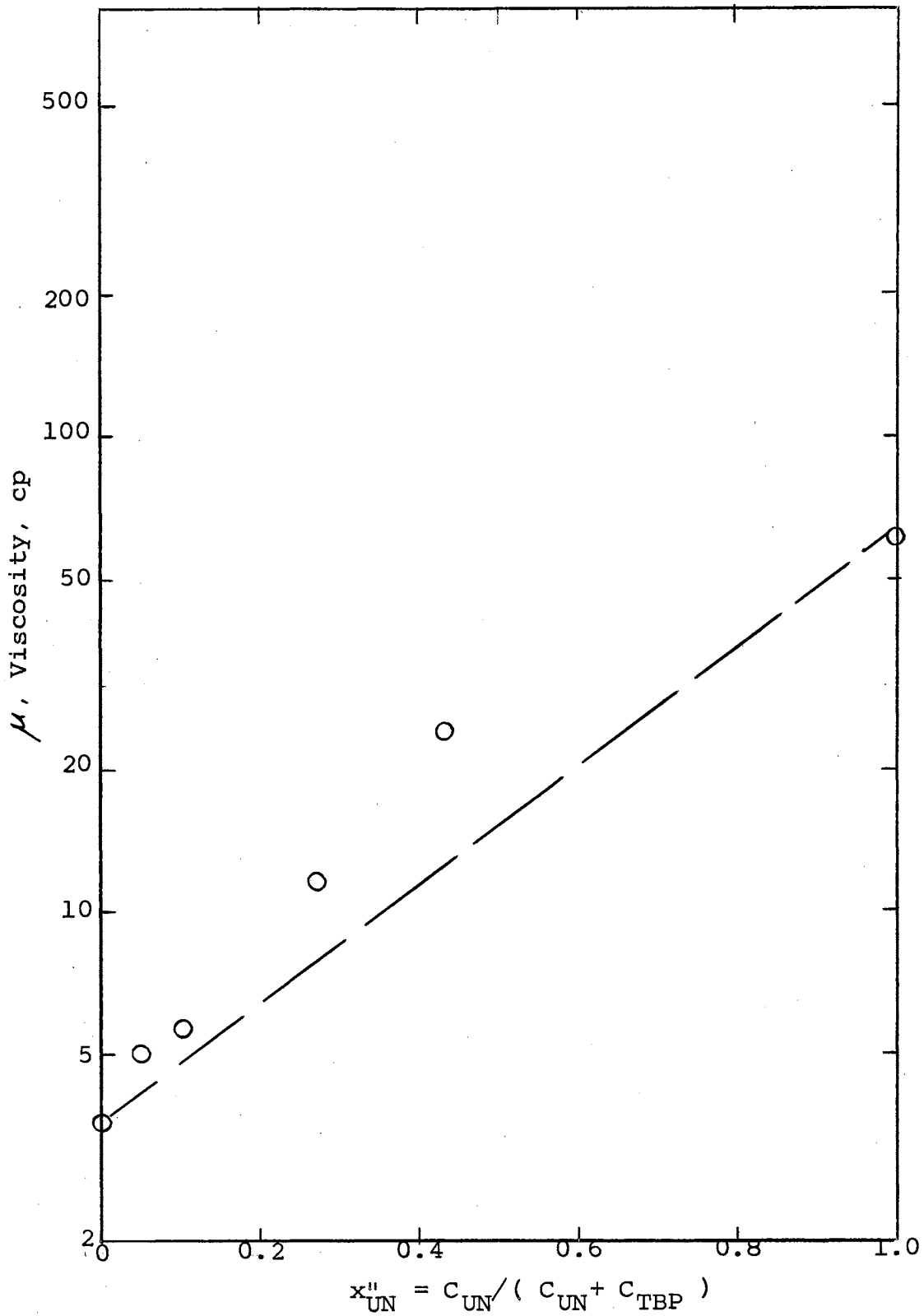

Figure 14. Variation of Solution Viscosity with Mole Fraction UN in the UN.2TBP–TBP Binary

The separate interaction effects in the binary system indicate no pronounced non-ideality or association between the components.

Comparison of the Diffusion Data with Empirical Correlations

At present many correlations for the prediction of dilute binary diffusion coefficients exist (58). Most of them are able to reproduce experimental diffusion data to within ± 20% or slightly better. For the system under study and from available thermodynamic data the correlations of Wilke-Chang (58), Scheibel (58) and Reddy et. al. (57) were chosen for comparison. The correlations were developed for the diffusion of a dilute specie, so only the experimental points at $\bar{C}_{UN} = 0.01$ can be tested. The solvent properties such as the molecular weight and the molar volume wherever required, were calculated from a mole fraction average of the solvent mixture of TBP and n-heptane. The association parameter in the Wilke-Chang correlation was taken as unity.

Table VIII shows that all of the correlations predict diffusion coefficients 30-50% higher than the observed values. The correlation by Reddy et. al. (57) shows the greatest deviation. The failure of the correlations may be attributed to the fact that all three correlations are based on diffusion data with greatest number of values that are an order of magnitude higher than those for the

TABLE VIII

COMPARISON OF DIFFUSION DATA
WITH EMPIRICAL CORRELATIONS

Solvent	Diffusion Coefficients x 10^6 cm^2/sec			
	Observed	Wilke-Chang	Scheibel	Reddy
100V/V%Heptane	8.171	12.0	13.5	17.1
30V/V%TBP	3.956	8.0	8.4	11.2
50V/V%TBP	3.053	5.8	5.7	7.9
70V/V%TBP	2.018	3.8	3.5	4.8
100V/V%TBP	0.826	1.9	1.6	2.3

uranyl nitrate system. The observed data represent points at one extreme end of the correlation.

All the literature data for the diffusion of uranyl nitrate in TBP (25, 30, 50) were with Amsco as diluent. No comparison between these and the above correlations can be made since all were taken at finite concentration with respect to uranyl nitrate.

A Generalized Plot of the Experimental Data: $\ln \frac{D\mu}{D_o\mu_o}$ vs. X_{UN}

The viscosity product $D\mu$, calculated from the experimental data at each TBP dilution, was studied with reference to the respective viscosity product at infinite dilution $D_o\mu_o$. The ratio $(D\mu/D_o\mu_o)$ for each system was plotted against the uranyl nitrate concentration, C_{UN}, as shown in Figure 15. The departure of the ratio $(D\mu/D_o\mu_o)$ from unity increases exponentially with the uranyl nitrate concentration. A smooth curve may be drawn through all the experimental data. The shape of the curve suggest an exponential relationship. Therefore the logarithm of $(D\mu/D_o\mu_o)$ was plotted against the mole fraction, C_{UN}, as shown in Figure 16. All the experimental data fall along a straight line with an average deviation of $\pm$ .07.

For some ideal binary systems, it had been shown (15)

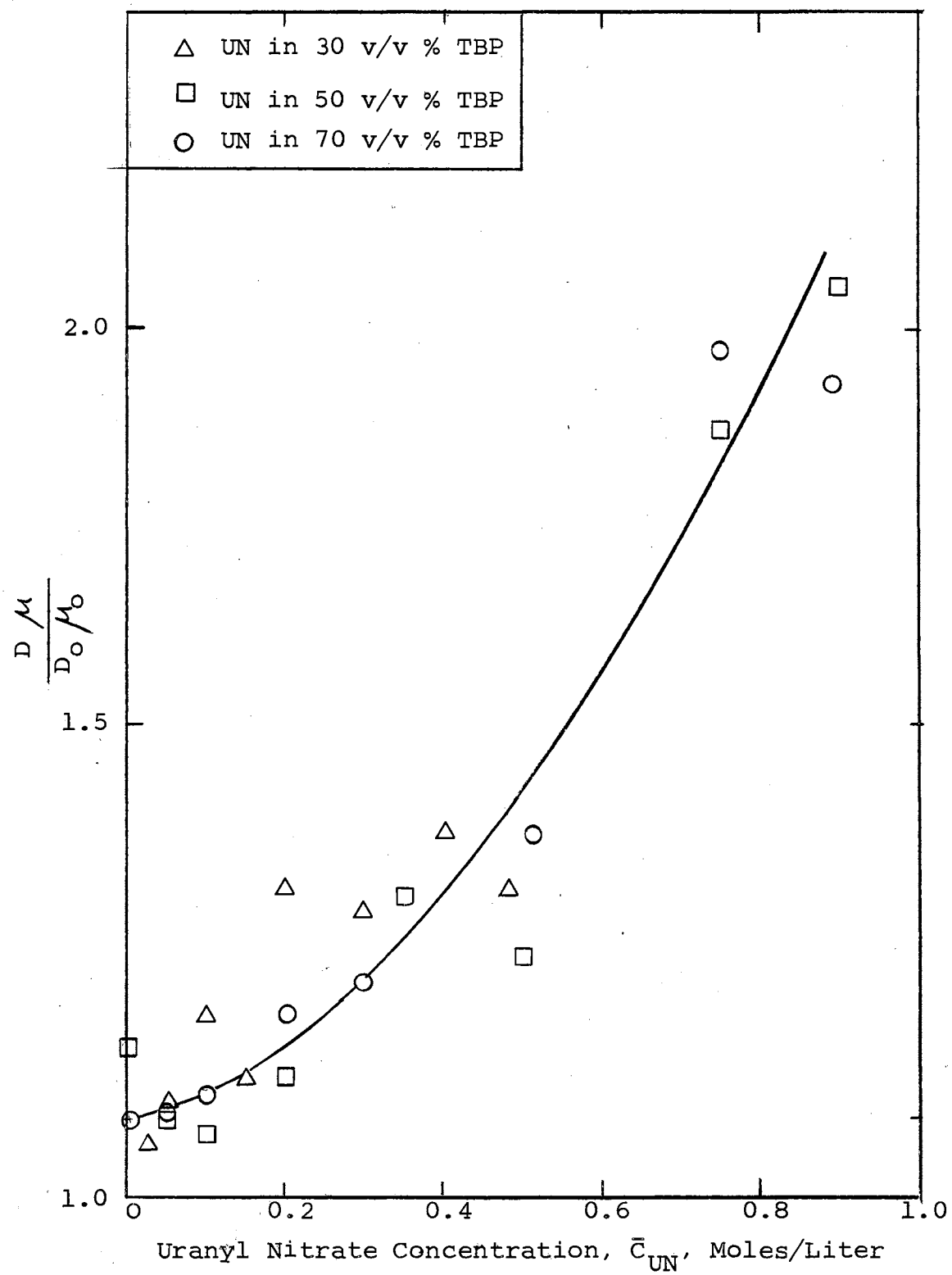

Figure 15. Variation of Diffusivity-Viscosity Product Ratio with Uranyl Nitrate Concentration

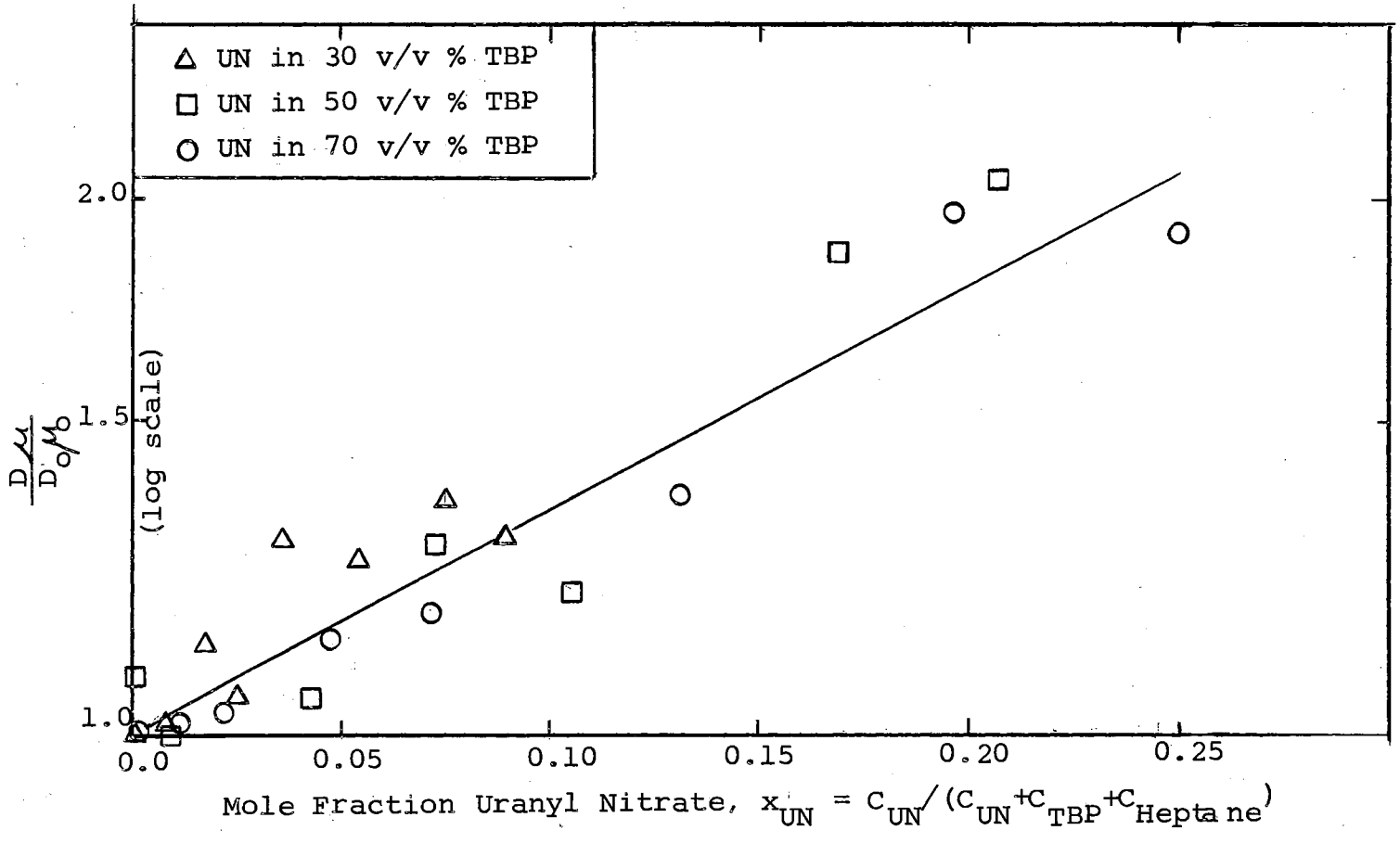

Figure 16. Variation of the Diffusivity-Viscosity Product Ratio with Mole Fraction Uranyl Nitrate (Water-Free Basis)

that D varies linearly with the mole fraction. The Hartley-Crank equation (31) which Bearman (4) had shown to be an expression for a regular binary solution also predicts the same linear relationship. The preceding discussion of the experimental data at the dilute region, has shown that the exponential behavior of D or $D\mu$ for the system studied here may be expected. But at finite concentrations of the solute, any of the simple treatment previously used may not be applicable. In the absence of the required activity data it is not possible to say, at this point, if the trends exhibited in Figure 15, and Figure 16, are due to the non-ideality of the solution or a valid trend for the transport and viscous processes. The generalized plot for all the experimental data is merely presented as an empirical relationship, without attempting to consider the theoretical implications. Such an empirical treatment may be useful for engineering purposes.

In the calculation of the mole fraction, C_{UN}, in the above plot, water was considered negligible or bonded to TBP. Both assumptions lead to almost equivalent numerical values of the mole fractions. Since there is no definite conclusion yet as to the nature of the water in the solution (60), it may be helpful to consider the extreme case when water is taken as an active component in the solution. No analytical data for the water content of the solution had been taken in this study. Water was calculated from the water solubility data given by Burger (14) for each

TBP dilution. In the presence of uranyl nitrate, it was assumed that the amount of water corresponds to the free TBP, in the same ratio of TBP/H_2O that was present in the original TBP-n-heptane mixture. Figure 17 shows a plot of $\ln(D\mu/D_o\mu_o)$ vs. the mole fraction with water included, X'''_{UN}. The same linear relationship may be inferred. The scatter of the data appear less, but this may not be considered a more valid treatment since the water content were not actual data but were assumed. It is noted that the presence of water does not seem to alter the shape of the curve.

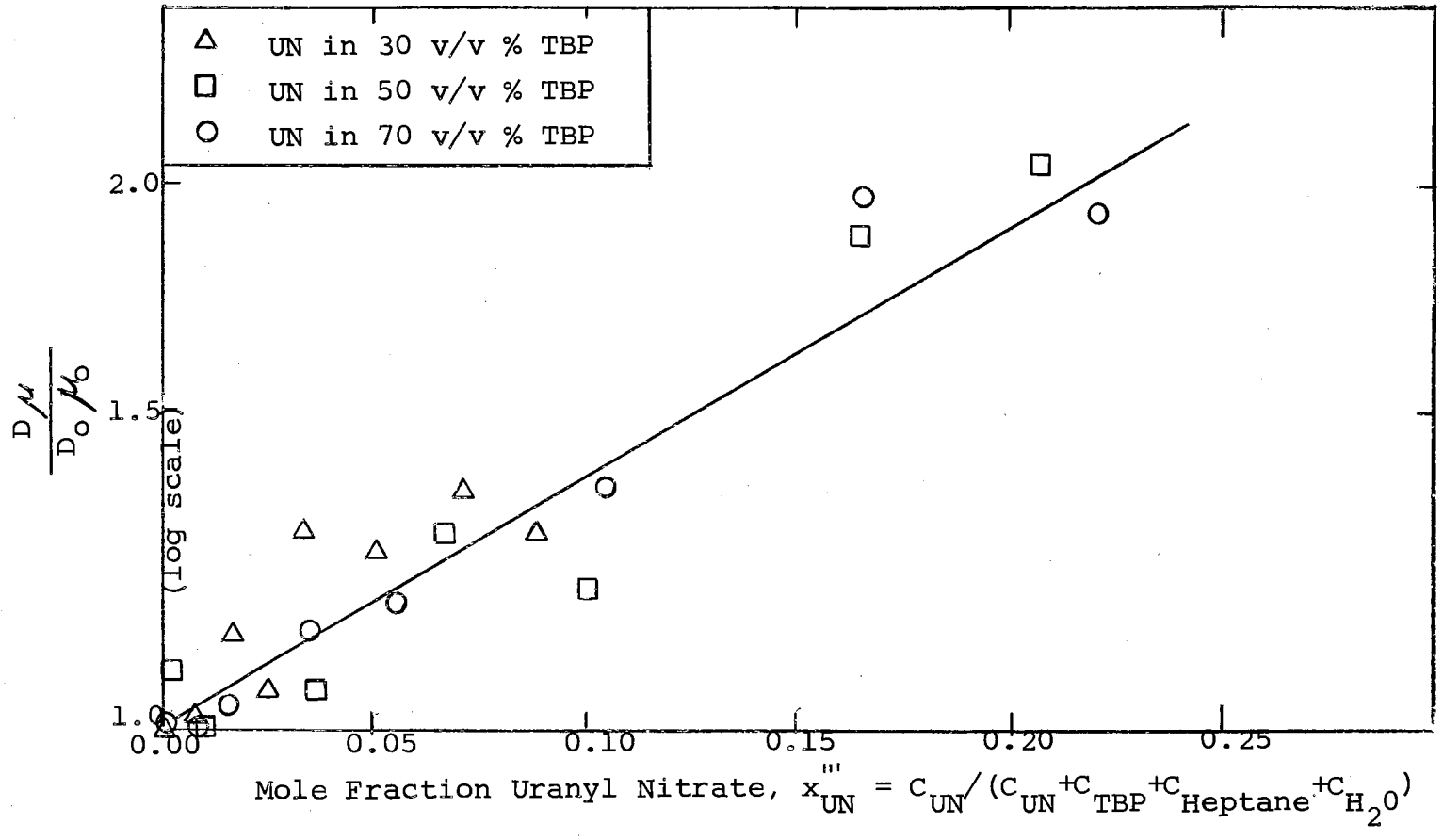

Figure 17. Variation of the Diffusivity-Viscosity Product Ratio with Mole Fraction Uranyl Nitrate (with Water)

CHAPTER VII

CONCLUSIONS AND RECOMMENDATIONS

In this study, experimental diffusion coefficient data were taken using a single Savart plate birefringent interferometer and a flowing junction diffusion cell. It was found, that the minimum initial concentration gradients to form the required fringe pattern, were .094 moles/l for aqueous NaCl solution and .02 moles/l for the organic uranyl nitrate solutions. On the average, successive diffusion runs of the same solution, yield diffusion coefficients which differ by $\pm$ .04 x 10^{-6} cm^2/sec. An analysis of error shows that the estimate of the standard error of D obtained from the curve fit provide a good approximation for the observed standard deviation.

The experimental data show that the diffusion of uranyl nitrate in the organic media is an order of magnitude slower than diffusion in aqueous solution. It was found that the diffusion coefficient decreases with uranyl nitrate concentration and increases with TBP dilution.

The experimental results and their comparison with the available theory show that in the very dilute uranyl nitrate range the organic diluent changes the solvent properties in the conventional manner of mole fraction

averages. In this range, the system could be treated as a pseudobinary and it may be inferred that only dispersion forces exist between the components of the system. The kinetic models of Olander (51) and of Vignes and Cullinan (18, 80), may be used for the prediction of effective diffusion coefficients for the uranyl nitrate-tributyl phosphate-n-heptane system at dilute uranyl nitrate concentrations.

Analysis of the viscosity data for the binary mixtures of $UO_2(NO_3)_2 \cdot 2TBP$-TBP, TBP-n-heptane and $UO_2(NO_3)_2 \cdot 2TBP$-n-heptane, indicate no significant interaction effects between the components.

At this point, no definite conclusion can be made about the diffusion coefficient at finite uranyl nitrate concentration, due to the absence of necessary thermodynamic data and a rigorous theory for multicomponent systems. It is simply observed that the diffusion coefficient exhibits a similar uranyl nitrate concentration dependence at the three TBP dilution studied.

For engineering purposes, a general correlation of a viscosity product ratio, $D\mu/D_o\mu_o$, as a function of the mole fraction of uranyl nitrate may be utilized with a reproducibility of $\pm$ .07.

With respect to the experimental procedure the following are recommended:

1. The present constant temperature bath should be

modified with the addition of a primary constant temperature bath in series with the bath containing the diffusion cell. The heating and the cooling elements and the stirrer should be put into this primary bath and the constant temperature liquid should be circulated between the primary and the secondary baths with a pump. The use of a liquid with higher heat capacity is also recommended. Such a set-up will nullify the rather large temperature changes encountered in diffusion runs of long duration as well as minimizing the vibrations in the cell bath which may cause disturbances at the interface.

2. Two important factors affect the magnitude of the estimate of the parameter D in the curve fit: the experimental error in the measurement of the distances between fringe pairs and the adequacy of the model, Equation (V-2) to represent the actual movement of the fringe pattern.

It is recommended that better methods of measurement of the distance between the fringes be studied. An example is the use of a photosensitive sensor other than a photographic film at the final image plane of the interferometer. The photosensitive device could allow direct quantitative evaluation of the distance between light intensity maxima or minima at predetermined time intervals. This method could eliminate certain limitations in measurement due to properties of photographic films such as, grain size and occasional poor contrast which was

shown to correlate with large diffusion coefficients. The time lag between an experimental run and the calculation of the diffusion coefficient caused by the procedures necessary in photographic analysis can also be decreased.

The model for diffusion as given by Equation (V-2) has been shown by Slater (71) to be adequate for evaluation of diffusion coefficients. However, the shape of the curve, or the model is very sensitive to the condition of the initial interface formed. Therefore, careful attention must be paid to keep the cell and the incoming solution free from particles that may clog the cell slits.

The following future work is recommended:

1. Further investigation of the nature of the water present in the solution is essential for a more rigorous theoretical treatment of the diffusion data. An analysis for the water content of the organic solution should be made.

2. Activity coefficient data for the system uranyl nitrate-TBP-n-heptane be taken.

3. To study further the influence of molecular interactions in diffusion, a diluent such as chloroform, which have been shown to form hydrogen bond with uranyl nitrate and TBP, be used.

SELECTED BIBLIOGRAPHY

1. Aartsen, J. J. and A. E. Karveze. Trans. Faraday Soc., 60, 510 (1964).

2. Apelbat, A. and A. Hornik. Trans. Faraday Soc., 63, 185 (1967).

3. Axtmann, R. C. Nucl. Sci. Eng., 16, 241 (1963).

4. Bearman, R. J. J. Phy. Chem., 65, 1961 (1961).

5. Beers, Y. Introduction to the Theory of Errors. Mass.: Addison-Wesley Publishing Co., p. 28 (1957).

6. Bird, B., W. Stewart and E. Lightfoot. Transport Phenomena. New York: J. Wiley and Sons, p. 513 (1960).

7. Box, G. E. P. and G. A. Coutie. Proc. Elec. Engrs., 103, Part B, Supp. No. 1, 100 (1956).

8. Bryngdahl, Olaf. Acta Chem. Scan., 11, 1017 (1957).

9. Bryngdahl, Olaf. J. Optical Soc. Am., 53, 571 (1963).

10. Bryngdahl, Olaf. and S. Ljunggren. J. Phy. Chem., 64, 1264 (196).

11. Burchard, J. K. and H. L. Toor. J. Phy. Chem., 66, 2015 (1962).

12. Burger, L. L. "The Decomposition Reactions of TBP and its Diluents," Progress in Nuclear Energy, Series III. Ed., F. Bruce, New York: Pergamon Press, p. 307 (1958).

13. Burger, L. L. US AEC Rpt. HW-19065 (1950).

14. Burger, L. S. and A. Forsmann. U.S. AEC Rpt. HW-20936 (1951).

15. Carman, P. C. and L. H. Stein. Trans. Faraday Soc., 52, 619 (1956).

16. Cosslet, Anna. J. Royal Microscopic Soc., 84, 385 (1965).

17. Crank, J. The Mathematics of Diffusion. Oxford: Clarendon Press, p. 9 (1957).

18. Cullinan, H. Ind. Eng. Chem. Fundamentals, 5, 281 (1966).

19. Cullinan, H. and M. Cusick. AI Ch. E.J., 13, 1171 1171 (1967).

20. Cullinan, H. and M. Cusick. Ind. Eng. Chem. Fundamentals, 6, 72 (1967).

21. Davis, W. and J. Mrochek. "Activities of TBP in TBP-Uranyl Nitrate-Water Solution." Solvent Extraction Chemistry. Ed. Dryssen, et. al., New York: Wiley, p. 283 (1967).

22. Dizdar, F. I. and D. Abrenovic. Proc. Intl. Conf. on Peaceful Uses of Atomic Energy, 28 (1958).

23. Dunlop, P. J. J. Phy. Chem., 68, 26 (1964).

24. Erbar, J. H. Private Communication. Oklahoma State University, Stillwater, Oklahoma (1968).

25. Finley, J. B., Ph.D. Thesis, Oklahoma State University (1964).

26. Fujita, H. J. Phy. Soc. Japan, 11, 1018 (1956).

27. Gainier, J. L. and A. B. Metzner. AICh. E.-I. Chem. E. Symp., Ser. No. 6, 74 (1965).

28. Glasstone, S., K. Laidler and H. Eyring. The Theory of Rate Processes. 1st ed. New York: McGraw Hill, p. 477 (1941).

29. deGroot, S. R. and P. Mazur. Non-equilibrium Thermodynamics. Amsterdam: North-Holland (1962).

30. Hahn, H. J. Am. Chem. Soc., 79 4625 (1957).

31. Hartley, G. S. and J. Crank. Trans. Faraday Soc., 45, 801 (1949).

32. Healy, T. V. AERE C/R-1772 (1956).

33. Healy, T. V. J. Inorg. Nucl. Chem., 19, 328 (1961).

34. Healy, T. V., J. Kennedy and G. Waind. J. Inorg. Nucl. Chem., 10, 137 (1959).

35. Healy, T. V. and H. A. McKay. Trans. Faraday Soc., 52, 533 (1956).

36. Holmes, J. et. al. AICh. E. J., 8, 646 (1962).

37. Ingelstaam, E. Arkiv For Fysik, 9, 197 (1955).

38. Ingelstaam, E. J. Am. Optical Soc., 47, 536 (1957).

39. Komarov, E. V. and Pushlenkov, M. F. Radiochemistry, 3, 56 (1961).

40. Laity, R. W. J. Phy. Chem., 63, 80 (1959).

41. Lau, E. and W. Krug. Die Aquidensitometrie, Berlin: Akademie Verlog (1957).

42. Libus, Z. J. Inorg. Nucl. Chem., 24, 619 (1962).

43. Lightfoot, E., E. Cussler and R. L. Tettig. AI Ch. E. J., 8, 708 (1962).

44. Marquardt, D. W. J. Soc. Ind. Appl. Math., 11, 431 (1963).

45. McKay, H. A. C. and T. V. Healy. "TBP as Extractant Solvent." Progress in Nuclear Energy. Series III Ed. F. Bruce, New York: Pergamon Press, p. 546 (1958).

46. Merliss, F., Ph.D. Thesis. University of Oklahoma (1968).

47. Moore, R. L. U.S. AECD-3196 (1951).

48. Nemodruk, A. A. and L. P. Glukhova. Russian J. Inorg. Chem., 8, 1370 (1963).

49. Nicolaev, A. V., et. al. Akad. Nauk SSSR Doklady, Chem. Sect., 155, 262 (1964).

50. Nicolaev, A. V., et. al. J. Structural Chem., 5, 449 (1964).

51. Olander, D. R. AICh. E. J., 9, 207 (1963).

52. Prigogine, I. Thermodynamics of Irreversible Processes. 2nd ed. New York: Interscience (1961).

53. Pushlenkov, M. F., et. al. Radiochemistry, 2, 27 (1960)

54. Pushlenkov, M. F., et. al. Radiochemistry, 4, 479 (1962).

55. Pushlenkov, M. F., et. al. Radiochemistry, 5, 496 (1963).

56. Pushlenkov, M. F. and O. N. Shuvalov. Radiochemistry, 5, 503 (1963).

57. Reddy, K. A. and L. K. Doraiswamy. Ind. Eng. Chem. Fundamentals, 6, 77 (1967).

58. Reid, R. and T. Sherwood, The Properties of Gases and Liquids, 2nd ed., New York: McGraw Hill, p. 543 (1966).

59. Robinson, R. A. and R. H. Stokes. Electrolyte Solutions, 2nd ed., London: Butterworths (1959).

60. Roddy, J. W. and J. Mrochek. J. Inorg. Nucl. Chem., 28, 3019 (1966).

61. Rozen, A. M. and N. Khorkhorina. Russian J. Inorg. Chem., 2, 389 (1958).

62. Rozen, A. M., et. al. Akad. Nauk SSSR Doklady, Phy. Chem. Sect., 153, 1147 (1963).

63. Sandquist, L. and P. Lyons. J. A. Chem. Soc., 76, 4641 (1954).

64. Shevchenko, V. B., et. al., Radiochemistry, 1, 126, (1960).

65. Shevchenko, V. B., et. al. Radiochemistry, 2, 77 (1961).

66. Sidall, T. H. J. Am. Chem. Soc., 81, 4176 (1959).

67. Siekierski, S. J. Inorg. Nucl. Chem., 24, 205 (1962).

68. Skinner, R. M., M. S. Thesis, Oklahoma State University (1964).

69. Skinner, R., Ph.D. Thesis, Oklahoma State University (1967).

70. Slater, C., M. S. Thesis, Oklahoma State University (1965).

71. Slater, C., Ph. D. Thesis, Oklahoma State University (1969).

72. Slansky, C. M., "The Properties of $UO_2(NO_3)_2$, $Al(NO_3)_2$, HNO_3 and H_2O System." Progress in Nuclear Energy, Series III, Ed. F. Bruce. New York: Pergamon Press, 535, (1958)

73. Strong, J. Concepts of Classical Optics, San Francisco: Witt, Freeman and Co., (1958).

74. Tang, Y. P. and D. Himmelblau. AICh. E. J., 11 54 (1965).

75. Taube, M. J. Inorg. Nucl. Chem., 15, 171 (1960).

76. Thomas, W. J. and E. M. Nicholl. Applied Optics, 4, (1965).

77. Trzebiatowska, J., et. al. J. Inorg. Nucl. Chem., 20, 106 (1961).

78. Tyrell, H. J. Diffusion and Heat Flow in Liquids, London: Butterworths (1961).

79. Vdovenko, V. M., et. al. Radiochemistry, 7, 137 (1965).

80. Vignes, Alain. Ind. Eng. Chem. Fundamentals, 5, 189 (1966).

APPENDIX A

TWO SAVART PLATE BIREFRINGENT INTERFEROMETER

At the initial phase of this study, an attempt was made to use the two Savart Plate arrangement (10) to measure diffusion coefficients. Figure 18 shows the optical arrangement for this system.

In the two Savart Plate method, the image obtained is the refractive index gradient along the direction of diffusion. The analytical expression is given by the solution to Fick's law of free diffusion (10,17). Measurements taken from the photographs were fitted to the equation to obtain the diffusion coefficients.

The reproducibilities obtained from this method were very poor. Furthermore, the skewness of the refractive index gradient curve could not be eliminated.

During this phase, a useful photographic development technique by Lau and Krug (41), suitable for accurate measurements from lines of finite width, was adopted. The technique is based on the so-called Sabattier-effect on photographic films to produce thin contour lines at either side of a fringe maximum.

L - LENS

P - POLARIZER

S - SAVART PLATE

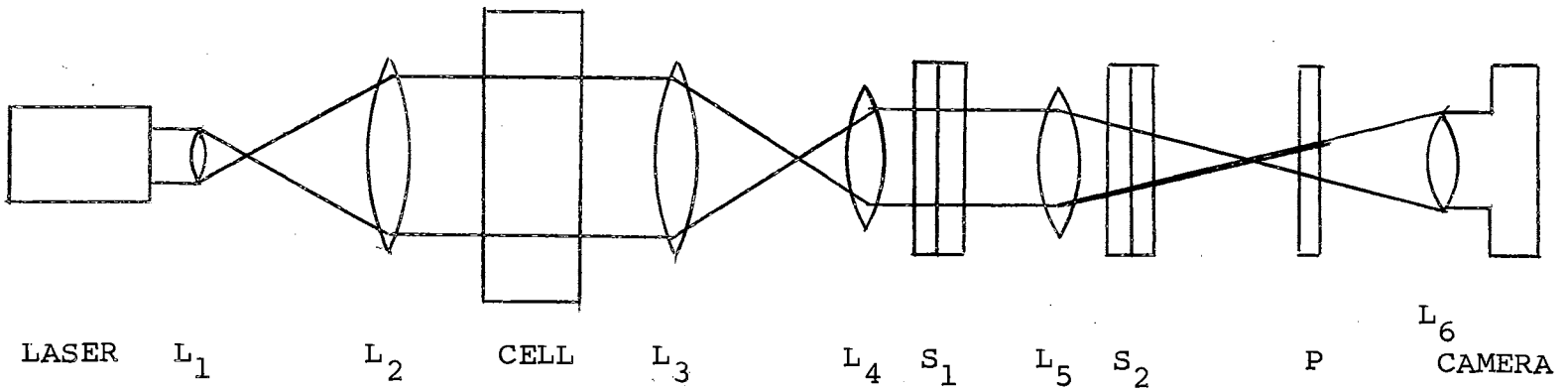

Figure 18. Two Savart Plate Interferometer

Equidensitometry

The procedure for producing equidensity lines by Cosslett (16) was adopted for the facilities in the laboratory. The materials used were Ilford N 60 photomechanical plates, a caustic hydroquinone developer (Ansco 70), an acid short stop bath, Kodak Fixer and Farmer's Reducer. For the second exposure, a 100 watt bulb attached to a safelight housing with white tracing paper as screen was used. This was attached to a voltage regulator set at 119 volts.

First, a high contrast copy of the original fringe pattern was made on the Ilford N 60 plate. This was accomplished by exposing the original film on top of the photomechanical plate held together between two glass plates, to a light flash (Honeywell Flash, 60 watts) held 6 ft. high and 3 ft. away from the plates. The plate was developed in the Ansco developer for $2\frac{1}{2}$ minutes, immersed in the stop bath for a second, washed in running water and then fixed for 2 minutes. The plate was then washed in running water and allowed to dry.

The developed plate was used to make a second contact copy on another Ilford plate. The two plates were exposed under the light flash held 6 ft. high and 9 ft. away. The second contact copy was put into the Ilford developer, removed after 100 seconds and washed in running water for 1 minute. It was then placed in a white flat dish,

completely covered with water, and placed under the diffuse light source, held 6 ft. away. The light was switched on for 10 seconds. The plate was put back into the developer for the rest of the normal developing time, immersed into a stop bath for a second and fixed for 2 minutes. After washing in running water the plate was reduced in the Farmers Reducer, fixed, finally washed and dried.

Figure 19 shows the original fringe pattern and the equidensity copy.

The above described photographic technique could be very useful in getting accurate measurements from fringe patterns. However, because of the number of steps involved, it is only practical for the case of the two-Savart plate birefringent interferometer, when one photograph can supply all the necessary data for the calculation of the diffusion coefficient. Bryngdahl (10) has mentioned some theoretical limitations of the method for use in evaluating fringe patterns.

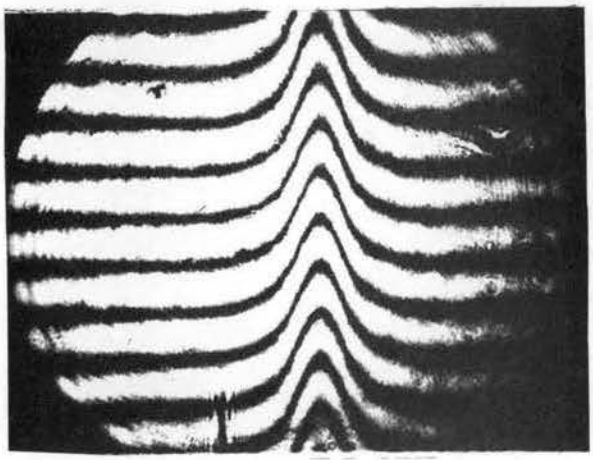

Photograph Developed by
Conventional Processing

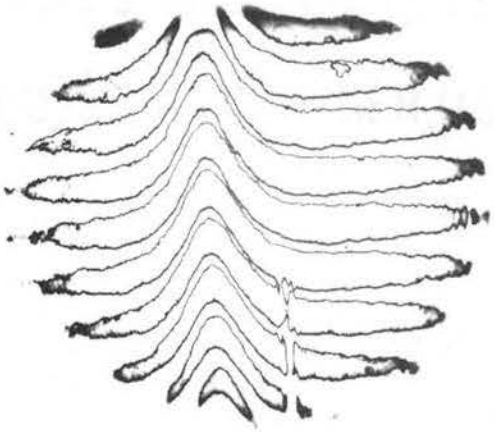

Photograph Processed by
Equidensitometric Method

Figure 19. Photographs for Diffusion Run Using Two Savart Plates

APPENDIX B

ERROR ANALYSIS

The derivations of the expressions used in the analysis of errors are given here.

The diffusion coefficient, D, is given by:

$$D = \frac{(2x)^2 MF}{8(t+\Delta t)\left(1 + \ln \frac{t_i + \Delta t}{t + \Delta t}\right)}$$

$$D = f(2x, t, \Delta t, t_i, T, MF) \qquad \text{(B-1)}$$

The fractional error in D was estimated using the statistical theory of error propagation (5), from the expression:

$$\frac{s_D}{D} = \sqrt{\frac{\left(\partial D/\partial(2x)\right)^2 s_{2x}^2}{D^2} + \frac{\left(\partial D/\partial(\Delta t)\right)^2 s_{\Delta t}^2}{D^2} + \frac{\left(\partial D/\partial(t_i)\right)^2 s_{t_i}^2}{D^2} + \frac{\left(\partial D/\partial MF\right)^2 s_{MF}^2}{D^2}} \qquad \text{(B-2)}$$

The individual terms in the equation are evaluated as follows:

$$\frac{\partial D}{\partial(\Delta t)} = \frac{(2x)^2 MF}{8(t+\Delta t)\left(1+\ln \frac{t_i+\Delta t}{t+\Delta t}\right)} \left[\frac{-1}{(t+\Delta t)} - \frac{1}{1+\ln \frac{t_i+\Delta t}{t+\Delta t}} \left(\frac{1}{t_i+\Delta t} - \frac{1}{t+\Delta t}\right)\right]$$

$$\frac{\partial D}{\partial(\Delta t)}\Big/ D = \left[\frac{1}{(t+\Delta t)} - \frac{1}{1+\ln \frac{t_i+\Delta t}{t+\Delta t}}\right]\left[\frac{1}{(t_i+\Delta t)} - \frac{1}{(t+\Delta t)}\right]$$

Near the top of the curve of $(2x)^2$ vs. t, the quantity $\left|\frac{t_i+\Delta t}{t+\Delta t}\right|$ does not vary much from unity. Since the calculations involve $(2x)^2$ and t data not far from this range it will be assumed that $\frac{t_i+\Delta t}{t+\Delta t}=1$ or $\ln\left|\frac{t_i+\Delta t}{t+\Delta t}\right|=0$. Therefore:

$$\frac{\partial D}{\partial \Delta t}\Big/D=\left[\frac{1}{(t+\Delta t)}-\left(\frac{1}{t_i+\Delta t}-\frac{1}{t+\Delta t}\right)\right] \qquad \text{(B-3)}$$

$$\approx\left|\frac{1}{t_i+\Delta t}\right|$$

Similarly:

$$\frac{\partial D}{\partial t_i}\Big/D \approx \frac{-1}{(t_i+\Delta t)\left(1+\ln\frac{t_i+\Delta t}{t+\Delta t}\right)} \qquad \text{(B-4)}$$

$$\approx \left|\frac{-1}{t_i+\Delta t}\right|$$

$$\frac{\partial D}{\partial MF}=\frac{(2x)^2}{8(t+\Delta t)\left(1+\ln\frac{t_i+\Delta t}{t+\Delta t}\right)} \qquad \text{(B-5)}$$

$$\frac{\partial D}{\partial MF}\Big/D=\frac{1}{MF}$$

The contribution of the magnification factor to Equation (B-12) is $\left|\frac{S_{MF}}{MF}\right|^2$. The calculation of this quantity is shown in later paragraphs.

Since the diffusion coefficient was obtained from a curve fit of $(2x)^2$ and t data, the contribution to the error, due to uncertainty in the measurement of 2x, was set equal to the estimate of the standard error of D in the curve fit, $\hat{S}_D$. The basic assumption here is that the equation or model is adequate to describe the experimental data. The estimate of the standard error of a parameter in a non-linear curve fit was calculated using the method

by Box (7). The method involves forming the matrix 2W whose elements S^{ij} are the partial second derivatives of the sum of squares $S(\Theta)$.

$$S(\theta) = \sum_{n}^{N} \left[Y_n - f(\chi, \theta) \right]^2 \tag{B-6}$$

$$S^{ij} = \left[\frac{\partial^2 S(\theta)}{\partial \theta_i \partial \theta_j} \right]_{\theta = \hat{\theta}} \tag{B-7}$$

The estimates of the variance and covariance of the parameters Θ are approximately the respective elements of the inverse matrix W^{-1} multiplied by the experimental error variance σ^2.

In terms of this study:

$$f(\chi, \theta) = 8\theta_1 (t + \theta_2)\left(1 + \ln \frac{\theta_3 + \theta_2}{t + \theta_2}\right) \tag{B-8}$$

$$S(\theta) = \sum \left\{ Y_n - 8\theta_1 (t_n + \theta_2) \left[1 + \ln \left(\frac{\theta_3 + \theta_2}{t_n + \theta_2} \right) \right] \right\}^2 \tag{B-9}$$

$$Z_n = (t_n + \theta_2)\left(1 + \ln \frac{\theta_3 + \theta_2}{t_n + \theta_2}\right) \tag{B-10}$$

$$\frac{\partial Z_n}{\partial \theta_2} \left(1 + \ln \frac{\theta_3 + \theta_2}{t_n + \theta_2}\right) + \left(t_n + \theta_2\right)\left(\frac{1}{\theta_3 + \theta_2} - \frac{1}{t_n + \theta_2}\right) \tag{B-11}$$

$$\frac{\partial Z_n}{\partial \theta_3} = (t_n + \theta_2)\left(\frac{1}{\theta_3 + \theta_2}\right) \tag{B-12}$$

$$\frac{\partial f_n}{\partial \theta_2} = 8\theta_1 \frac{\partial Z_n}{\partial \theta_2} \tag{B-13}$$

$$\frac{\partial f_n}{\partial \theta_3} = 8\theta_1 \frac{\partial Z_n}{\partial \theta_3} \tag{B-14}$$

$$\frac{\partial^2 Z_n}{\partial \theta_2^2} = 2\left(\frac{1}{\theta_3+\theta_2} - \frac{1}{t_n+\theta_2}\right) + (t_n+\theta_2)\left[\frac{1}{(\theta_3+\theta_2)^2} + \frac{1}{(t_n+\theta_2)^2}\right] \tag{B-15}$$

$$\frac{\partial^2 f_n}{\partial \theta_2^2} = 8\theta_1 \frac{\partial^2 Z_n}{\partial \theta_2^2} \tag{B-16}$$

$$\frac{\partial^2 Z_n}{\partial \theta_2 \partial \theta_3} = \frac{1}{(\theta_3+\theta_2)} + (t_n+\theta_2)\left[\frac{-1}{(\theta_3+\theta_2)^2}\right] \tag{B-17}$$

$$\frac{\partial^2 f_n}{\partial \theta_2 \partial \theta_3} = 8\theta_1 \frac{\partial^2 Z_n}{\partial \theta_2 \partial \theta_3} \tag{B18}$$

$$\frac{\partial^2 Z_n}{\partial \theta_3^2} = \left[\frac{-1}{(\theta_3+\theta_2)^2}\right]\left[t_n + \theta_2\right] \tag{B19}$$

$$\frac{\partial^2 f_n}{\partial \theta_3^2} = 8\theta_1 \frac{\partial^2 Z_n}{\partial \theta_3^2} \tag{B-20}$$

The expressions for the elements of the matrix are:

$$S'' = \left[\frac{\partial^2 S}{\partial \theta_1^2}\right]_{\theta=\hat{\theta}} = \sum_n^N 128 (Z_n)^2 \tag{B-21}$$

$$S^{12} = \left[\frac{\partial^2 S}{\partial \theta_1 \partial \theta_2}\right]_{\theta=\hat{\theta}} = \sum_n^N \left\{ -16 Y_n \frac{\partial Z_n}{\partial \theta_2} + 16 Z_n \frac{\partial f_n}{\partial \theta_2} + 16 f_n \frac{\partial Z_n}{\partial \theta_2} \right\} \tag{B-22}$$

$$S^{13} = \left[\frac{\partial^2 S}{\partial \theta_1 \partial \theta_3}\right]_{\theta=\hat{\theta}} = \sum_n^N \left\{ -16 Y_n \frac{\partial Z_n}{\partial \theta_3} + 16 Z_n \frac{\partial f_n}{\partial \theta_3} + 16 f_n \frac{\partial Z_n}{\partial \theta_3} \right\} \tag{B-23}$$

$$S^{22} = \left[\frac{\partial^2 S}{\partial \theta_2^2}\right]_{\theta=\hat{\theta}} = \sum_n^N \left\{ -16 Y_n \theta_1 \frac{\partial^2 Z_n}{\partial \theta_2^2} + 2\left(\frac{\partial f_n}{\partial \theta_2}\right)^2 + 2 f_n \frac{\partial^2 f_n}{\partial \theta_2^2} \right\} \tag{B-24}$$

$$S^{23} = \left[\frac{\partial^2 S}{\partial \theta_2 \partial \theta_3}\right]_{\theta=\hat{\theta}} = \sum_n^N \left\{ -16 Y_n \theta_1 \frac{\partial^2 Z_n}{\partial \theta_2 \partial \theta_3} + 2\left(\frac{\partial f_n}{\partial \theta_3} \frac{\partial f_n}{\partial \theta_2}\right) + 2 f_n \frac{\partial^2 f_n}{\partial \theta_2 \partial \theta_3} \right\} \tag{B-25}$$

$$S^{33} = \left[\frac{\partial^2 S}{\partial \theta_3^2}\right]_{\theta=\hat{\theta}} \sum_n^N \left\{ -16 Y_n \theta_1 \frac{\partial^2 Z_n}{\partial \theta_3^2} + 2\left(\frac{\partial f_n}{\partial \theta_3}\right)^2 + 2 f_n \frac{\partial^2 f_n}{\partial \theta_3^2} \right\} \tag{B-26}$$

$$2W = \begin{vmatrix} S^{11} & S^{12} & S^{13} \\ S^{21} & S^{22} & S^{23} \\ S^{31} & S^{32} & S^{33} \end{vmatrix} \qquad \begin{aligned} S^{12} &= S^{21} \\ S^{13} &= S^{31} \\ S^{23} &= S^{33} \end{aligned} \qquad \text{(B-27)}$$

$$W^{-1} = \begin{vmatrix} A^{11} & A^{12} & A^{13} \\ A^{21} & A^{22} & A^{23} \\ A^{31} & A^{32} & A^{33} \end{vmatrix} \qquad \text{(B-28)}$$

$$\begin{aligned} \hat{S}_{\theta_1=D} &= A^{11}\sigma^2 \\ \hat{S}_{\theta_2=\Delta t} &= A^{22}\sigma^2 \\ \hat{S}_{\theta_3=t_i} &= A^{33}\sigma^2 \end{aligned} \qquad \text{(B-29)}$$

The values of the experimental error variance σ, used were the final sum of squares obtained from the curve fit divided by the number of observations N. All the calculations were carried out in an IBM 360 computer. Typical values obtained were as follows:

Run Number	$\hat{S}_{\theta_1=D}$	$\hat{S}_{\theta_2=\Delta t}$	$\hat{S}_{\theta_3=t_i}$
7C2	$.0068\times10^{-6}$	3.79	1.71
7C1	$.0070\times10^{-6}$	4.5	2.05
7C3	$.0075\times10^{-6}$	4.05	1.80
3I4	$.0496\times10^{-6}$	6.19	2.08
3I5	$.0396\times10^{-6}$	5.37	1.93
5A4	$.0527\times10^{-6}$	7.25	4.72
5A3	$.0342\times10^{-6}$	5.65	3.42

The final expression for Equation (B-2) is:

$$\frac{S_D}{D} = \sqrt{\left(\frac{\hat{S}_{\theta_i=D}}{D}\right)^2 + \left(\frac{S_{\Delta t}}{t_i+\Delta t}\right)^2 + \left(\frac{S_{t_i}}{t_i+\Delta t}\right)^2 + \left(\frac{S_{MF}}{MF}\right)^2} \qquad \text{(VI-1)}$$

The standard error of Δt ($s_{\Delta t}$) and ti (s_{ti}) were estimated from the difference in the Δt and ti respectively, obtained from diffusion runs of identical solutions, As will be shown in later paragraphs, the quantity $\frac{S_{MF}}{MF} = .0043$. Therefore, for the representative runs below:

For Run 7C:

$$\frac{S_D}{D} = \sqrt{\left(\frac{.007}{1.5}\right)^2 + \left(\frac{7}{1050}\right)^2 + \left(\frac{30}{1050}\right)^2 + (.0043)^2} = .03$$

For Run 3I:

$$\frac{S_D}{D} = \sqrt{\left(\frac{.045}{3.6}\right)^2 + \left(\frac{8}{550}\right)^2 + \left(\frac{30}{550}\right)^2 + (.0043)^2} = .05$$

For Run 5A:

$$\frac{S_D}{D} = \sqrt{\left(\frac{.04}{2.8}\right)^2 + \left(\frac{20}{630}\right)^2 + \left(\frac{10}{630}\right)^2 + .0043} = .03$$

The same procedure as above was used to estimate the fractional error in the magnification factor MF. In this case:

$$MF = \frac{8D(t+\Delta t)\left(1+\ln\frac{t_i+\Delta t}{t+\Delta t}\right)}{(2x)^2} \qquad \text{(B-33)}$$

$$\frac{S_{MF}}{MF} = \sqrt{\left(\frac{\hat{S}_{MF}}{MF}\right)^2 + \left(\frac{S_{\Delta t}}{t_i+\Delta t}\right)^2 + \left(\frac{S_{t_i}}{t_i+\Delta t}\right)^2} \qquad \text{(B-34)}$$

It was found that the contribution to the error due to boundary formation ($s_{\Delta t}$ and s_{ti}) were negligible. The error was determined by the estimate of the variance of the parameter MF in the curve fit, as obtained also by the method of Box (7).

$$\frac{S_{MF}}{MF} = \sqrt{\left(\frac{\hat{S}_{MF}}{MF}\right)^2} = \frac{.00199 \times 10^{-2}}{.4622 \times 10^{-2}} = .0043 \qquad \text{(B-35)}$$

An independent estimate of the magnification factor was also obtained as follows:

Cell cavity width actual measurement - 0.229 inches

Image of cell cavity width read at at Vanguard Motion Analyzer - 8.504 inches

$$MF = \left(\frac{0.229}{8.504} \times 2.54\right)^2 = .004678 \qquad \text{(B-36)}$$

MF from diffusion runs = .0046139

% DEV = 1.4%

APPENDIX C

CALCULATIONS FOR THE MODIFIED ABSOLUTE RATE THEORY OF DIFFUSION

The calculation of the group $\underline{Y}$ and the activation energy term δ from the modified absolute rate theory of Olander (51) is presented here.

$$Y = \left(\frac{D\mu}{T}\right)\left(\frac{\xi}{K}\right)\left(\frac{V}{N_{av}}\right)^{1/3} = exp\left[\frac{\Delta G_\mu - \Delta G_D}{RT}\right] \qquad \text{(II-20)}$$

$$f\delta = \frac{\Delta G_\mu - \Delta G_D}{RT}$$

$$\delta = \left(\frac{\Delta G_{AA}}{RT}\right)\left[1 - \left(\frac{\Delta G_{ss}}{\Delta G_{AA}}\right)^{1/2}\right] \qquad \text{(II-24)}$$

$$\frac{\Delta G}{RT} = ln\left[\frac{\mu V}{h N_{AV}}\right] \qquad \text{(II-25)}$$

For the system under study, the physical properties used in the calculation of the free energy ΔG are:

	TBP	Heptane	$UO_2(NO_3)_2 \cdot 2TBP$
μ(cp)	.0399	.0039	61.2
V $\frac{cm^3}{g\text{-mole}}$	274	147	606

Using these values in Equations (II-25) and (II-24) the following quantities were obtained:

	TBP	Heptane	$UO_2(NO_3)_2 \cdot 2TBP$
$\Delta G/RT$	7.9	4.95	11.45
δ	-1.58	-2.57	-

Equation (II-20) was extended to the case of the diffusion of a dilute specie in a mixture of solvents by using mole fraction averages for the variables V and . The mole fractions were calculated on a solute free basis (since the solute is present in very low concentrations) and assuming that there is no free water present in the solution.

$$X_T + X_H = 1.0$$

$$V_m = X_T V_T + X_H V_H \qquad \text{(C-1)}$$

$$\delta_m = X_T \delta_T + X_H \delta_H$$

Using the experimental diffusion and viscosity data, the following values were obtained.

δ_m	Y
-2.57	0.290
-2.40	0.245
-2.23	0.290
-2.04	0.357
-1.58	0.396

NOMENCLATURE

a_i	-	Activity of component i, mole fraction units
A^{ij}	-	Elements of the inverse matrix W^{-1}
B	-	A constant defined by Equation (II-48)
C	-	Total molar concentration, moles/liter
C_i	-	Concentration of somponent k, moles/liter
$\mathcal{D}_{ij}$	-	Binary diffusion coefficient, cm^2sec^{-1}
D	-	Diffusion coefficient defined by Equation (II-6), cm^2/sec^{-1}
D'	-	Diffusion coefficient defined by Equations (V-6) and (V-7), cm^2sec^{-1}
D_{lm}	-	Effective diffusion coefficient in a multi-component system, cm^2sec^{-1}
D*	-	Multicomponent diffusion coefficient defined Equation (II-46), cm^2sec^{-1}
F_{ij}	-	Friction coefficient, defined by Equation (II-28)
f	-	Fraction of the total free energy of activation due to the bond breaking step
$f(\chi, \Theta)$	-	Theoretical model used in the curve fit, Equation (B-8)
ΔG	-	Free energy of activation, cal/mole
h	-	Planck's constant, 6.624×10^{-27} erg-sec
J_i	-	Rate of transfer of component i with respect to the volume average frame of reference defined by Equation (V-7), $moles/cm^2sec$
K	-	Reaction equilibrium constant, concentration units
K_D	-	Uranyl nitrate distribution ratio defined by Equation (II-4)

k - Boltzmann constant, 1.38×10^{-16} erg/°K

k' - Rate constant from the Absolute Rate Theory

L - Number of component

M - Molecular weight, gm/g-mole

MF - Magnification factor

N_1 - Rate of transfer of the diffusing component, per unit area across the interface, defined by Equation (II-5a), moles/cm^2sec

N - Number of data points

N_{av} - Avogadro's constant, 6.023×10^{23}

R - gas constant, cal/mole °K

r_i - Radius of molecular specie i, cm

s - Standard deviation

$S(\Theta)$ - Estimate of the standard error of the parameter Θ_i obtained in the curve fit

S^{ij} - Elements of the matrix 2W defined by Equation (B-7)

T - Temperature, °K

t - Diffusion time, sec

t_i - Time corresponding to maximum separation between fringes, sec

Δt - Time correction for a finite interface, sec

$\bar{V}_i$ - Partial molar volume of component i, cm^3/g-mole

v_i - Velocity of component i, cm/sec

V_i - Molar volume of component i, cm^3

v^o - Bulk velocity of the solution, cm/sec

V_f - Free volume in the Eyring theory, cm^3

W - Matrix defined by equation (B-27)

W^{-1} - Inverse matrix defined by Equation (B-27)

x - Space coordinate measured normal to the interface

$2x$ - Distance between the next to the outermost fringe pair, cm.

X_i - Mole fraction of component i

X_{UN} - Mole fraction defined by: $\frac{C_{UN}}{C_{UN}+C_{TBP}+C_{Heptane}}$

X'_{UN} - Mole fraction defined by: $\frac{C_{UN}}{C_{UN}+C_{Heptane}}$

X''_{UN} - Mole fraction defined by: $\frac{C_{UN}}{C_{UN}+C_{TBP}}$

X'''_{UN} - Mole fraction defined by:

$$\frac{C_{UN}}{C_{UN}+C_{TBP}+C_{Heptane}+H_2O}$$

X_H - Mole fraction n-heptane in the TBP-n-heptane binary

Y - Dimensionless group defined by Equation (II-20)

Y_n - Experimental $(2x)^2$ data, cm^2

Z_n - A group defined by Equation (B-10)

u_i - Chemical potential of component i

$Z(x,t)$ - optical path representation

Subscripts:

1 - Denote solute

2 - Denote solvent

3 - Denote another solvent component

m - Mixture of solvents

μ - Viscous process

D - Diffusive process

i,j,k - Components in solution

n - nth observation

o - Denotes at the composition extrema

Superscript:

j - Bond breaking step

h - hole forming step

AA - Interaction between solvent molecules

SS - Interaction between solute molecules

AS - Interaction between solute and solvent molecule

o - Denotes at the composition extrema

Greek symbols:

α - Parameter with a dimension of length used in the Hartley-Crank diffusion equation

γ - Activity coefficient of component i

$\gamma_{\pm}$ - Mean activity coefficient of the ions in the aqueous solution

α_{ij}^{k} - Thermodynamic parameter used in the multi-component diffusion theory of Cullinan

δ - Activation energy term defined by Equation (II-24)

Δ - Change in a variable

ζ - Flow resistance term defined by Equation (II-10)

ζ_{ij} - Friction coefficient defined by Equation (II-34)

Θ - Parameter in the curve fit

λ - Jump length in Eyring's Absolute Rate Theory, cm

μ_i - Viscosity of component i, centipoise

μ_{12} - Viscosity of binary mixture, centipoise

ρ - Density, gm/cm^3

Π - Product sign

π - Constant

$\sum$ - Summation sign

χ - Used to represent variables in the curve fit

ξ - Parameter in Eyring's theory

σ^2 - Variance

VITA

Amable Dorotan Hortaçsu

Candidate for the Degree of

Doctor of Philosophy

Thesis: DILUENT EFFECTS ON DIFFUSION FOR THE SYSTEM URANYL NITRATE-TRIBUTYL PHOSPHATE-N-HEPTANE

Major Field: Chemical Engineering

Biographical:

Personal Data: Born in Irosin, Sorsogon, Philippines, May 7, 1942, the daughter of Vicente and Beata Dorotan, married to Öner Hortaçsu, Stillwater, Oklahoma, June 7, 1968.

Education: Attended elementary school in Irosin Central School; graduated from Irosin High School in 1958; received the Bachelor of Science degree in Chemical Engineering from the University of the Philippines in 1963; received the Master of Science degree with a major in Chemical Engineering from Oklahoma State University in May, 1965; completed the requirements for the Doctor of Philosophy degree, July 31, 1970.